NASA CR-159,021

NASA CONTRACTOR REPORT 159021

NASA-CR-159021
19790011889

JOVIAN PROBE WAKE FLOWFIELD

CARL D. ENGEL
REMTECH INC.
HUNTSVILLE, AL 35805

CONTRACT NAS1-15446
MARCH 1979

NASA
National Aeronautics and
Space Administration

Langley Research Center
Hampton, Virginia 23665
AC 804 827-3966

FOREWORD

This final report presents work which was conducted for Langley Research Center (LaRC) in response to requirements of Contract NAS1-15446. The work presented was performed at REMTECH's Huntsville office and is entitled "Jovian Probe Wake Flowfield Study."

The NASA technical coordination for this study was provided by Dr. James Moss of the Aerothermodynamics Branch of the Space Systems Division.

TABLE OF CONTENTS

LIST OF TABLES

LIST OF FIGURES

NOMENCLATURE

a	Term defined in Equation 4; also, sonic velocity
A	Area
AF	Air Force
ANSI	American National Standards Institute
ASCII	American Standard Computer Interchange Institute
b	Scale factor in far wake shape - see Equation 2
BPI	Bits Per Inch
c_p	Specific heat at constant pressure
C_D	Drag coefficient
CEC	Chemical Equilibrium Composition
CESL	Chemical Equilibrium Shear Layer
d	Diameter of probe
F	Fraction of internal species mixed with external species
H	Enthalpy
HYVIS	Hypersonic viscous shock layer program
m	Exponent term in far wake shape -see Equation 2
M	Mach number
$\overline{M}$	Molecular weight
MOC	Method Of Characteristics
n	Term defining two-dimensional or axisymmetric flow
O/F	Oxider to fuel ratio
P	Pressure
r	Radial distance from axis of symmetry
R	Gas constant; also, Radius of probe

Re	Reynolds number based on freestream conditions and body diameter
T	Temperature
u,U	Velocity
x	Axial distance from aft end of body
X	Axial distance from probe shoulder
y	Radial distance from axis of symmetry
Y	Mole fraction
γ	Ratio of specific heats
δ^*	Boundary layer displacement thickness
ΔY	Width of mixing region
Θ	Angle
μ	Viscosity
ρ	Density
ψ	Stream function defined in Equation 5

Subscripts

B	Base
c	Cone
d	Diameter of probe
e	Edge of boundary layer
N	Neck
o	Stagnation
r	Reference
s	Static; also, Shock
∞	Freestream conditions

Section 1.0

INTRODUCTION

In January, 1982, the Galileo Spacecraft consisting of a Jupiter orbiter and probe is scheduled for launch. After planetary arrival, the probe will enter Jupiter's atmosphere with a relative entry velocity of 48 km/sec. In order for the probe to survive the severe aerothermal entry conditions a large portion of the probe's weight must be delegated to the thermal protection system. Until very recently the primary thrust of the design and analysis work has been concentrated on the forebody thermal environment. The forebody shock layer produces temperatures in the 10,000 to 20,000 K range. This produces a radiative heating dominated environment coupled to massive ablation into the shock layer, Ref. (1 and 2). The ablation products from the forebody shock layer are dumped into the probe's wake.

Recently, attention has begun to focus on the probe's wake to assess the heating input into the base region of the probe. This study addresses one major aspect of the base heating problem. In order to calculate the radiative heating to the base region of the Jovian probe, the entire wake flowfield must be defined. This study addresses the development and use of engineering tools for calculating the probe's wake flowfield.

The specific objective of this study was to calculate the near and far viscous and inviscid flowfields for three entry conditions. The flowfields were to include pressure, temperature and species concentration for radiation analysis work. These flowfields were calculated radially for 2.5 body radii and axially for 10 body radii. The results obtained indicate that temperatures in the Jovian probe wake will range from 4,000 to 10,000 K and pressures will range from 10 to 1,000 times the free-stream value. Section 2 of this report describes the math model used in the calculations. Section 3 provides a description of the results, and this is followed by conclusions and recommendations in Section 4.

Section 2.0

WAKE FLOWFIELD MODEL

In keeping with the objectives of this study an engineering model was developed for the Jovian probe wake flowfield. The different regions of the flowfield are shown schematically in Fig. 1. The gas state properties and the models for each of the regions shown in Fig. 1 are discussed in detail in the following subsections.

2.1 Thermodynamics

Equilibrium thermodynamic properties were used throughout this study. The curve fit coefficients for heat capacity, enthalpy and entropy were obtained from Moss (Private communications from James Moss, NASA Langley Research Center, Hampton, Virginia) for use in the chemical equilibrium composition (CEC) program (Ref 3). Two ranges of thermodynamic property curve fits were used (1000 K to 6000 K and 6000 K to 16000 K). The CEC program determines the equilibrium composition of a gas mixture by minimization of Gibbs free energy.

The three flight cases analyzed during this study are specified in Table 1. Case 1 and 2 are documented in Ref. 1 and Case 3 was obtained from Moss. Computer printout from the HYVIS program (Ref. 1) were obtained for all three cases. Thermodynamic property output from the Langley HYVIS program were compared with the use of the CEC program in this study. These results are shown in Tables 2a, b and c for Cases 1, 2 and 3 respectively. The temperature, pressure and elemental composition were specified and all other properties were computed by the CEC program. The results are for three shock layer conditions and are in excellent agreement for all variables.

The CEC program was used to supply thermodynamic property information to the flowfield math models used in the wake. To accomplish this several options were used:

RKT - Constant entropy expansion from specified total conditions

T,P - Specified temperature and pressure

H,P - Specified enthalpy and pressure

Throughout the analysis six species were considered in the inviscid flowfield and nineteen species were considered in the viscous flowfields.

2.2 Inviscid Near Wake

The inviscid near wake flowfield was calculated using an axisymmetric method of characteristics (MOC) solution with boundary conditions on the viscous shear layer side of the flowfield defined by empirical means. The MOC solution will be discussed followed by a discussion of the viscous wake neck location and viscous near wake pressure boundary.

MOC

The axisymmetric MOC code of Ref. (4) was used to calculate the flow properties of all of the inviscid regions. An especially desirable feature of that code was the capability to handle real gas properties in the calculation. However, there were several modifications necessary to perform the Jovian probe study. Three changes were mandatory to obtain diagnostic-free output, and one improvement significantly facilitated usage. When these advancements were incorporated, relatively straightforward production of the desired cases was practical.

Two of the three mandatory changes were related to the real gas properties. One was a significant increase in the amount of gas properties stored, and one was a logic change related to reference (ideal) gas conditions. The Ref. (4) code had been set up for gas properties defined in a matrix of up to thirteen velocity values at each of two entropy values, at each of ten oxidizer-to-fuel (O/F) ratio values. However, the very wide spectrum of entropies and velocities associated with the Jovian probe led to a need for thirty velocity values at each of thirty entropy cuts. There was no need for any variation in O/F ratio (a rocket engine characteristic). By adroit modification of the internal storage, the improved code was able to operate using the same size computer storage as before.

The third necessary change resulted from the unusually high Mach number values of this study. In the gas properties lookup sequence, a maximum velocity had been calculated as

$$U_{max} = 0.999 \sqrt{2\gamma R T_o/(\gamma-1)}$$

The scale factor had to be increased from 0.999 to 0.9995 to preclude erroneous operation.

An addition was made to the code to facilitate usage. The original code printed the flowfield as it was calculated; thus, the great bulk of the output data made it tedious to rapidly locate especially pertinent data, such as along boundaries. A subroutine was written to store and later print a summary of flow properties along the shocks, along the vehicle wall, and along any free boundary (constant-pressure surface). In addition, an auxiliary program was written to generate card input to the MOC code, for the far viscous wake quartic surface which was approximated as 100 straight-line segments.

The near wake inviscid flowfields were calculated with the MOC using a conical forebody and a short cylinder section. This was followed by a constant pressure boundary to the viscous neck axial station.

Wake Shape

The wake structure for this probe is considered to be generally as sketched in Fig. 1. To initiate this study, it was first necessary to estimate the geometric extent or shape of the viscous portions of this wake: the free shear layer and the inner far wake. Analytical means were not available, and an experimental approach was beyond the allowable resources. An empirical correlation approach was deemed appropriate. That is, available experimental data were used to estimate the shape of the nominal wake edge. The success of this approach depends on the applicability of the test data to the Jovian probe conditions. The conditions assumed were:

$$M_\infty = 40$$

$$Re_{\infty d} = 10^6$$

Shape of Galileo Probe vehicle (Fig. 1)

The wake shape was desired for approximately the first six probe diameters downstream.

It was initially planned to use a four-step procedure. First, the wake shape downstream of the neck would be established by the theory of Lees (Ref. 5). Second, the neck location would be approximated by the Reeves and Lees technique (Ref. 6). Third, combining this location with the Lees shape would set the neck diameter. Finally, this diameter would be connected to the probe shoulder by straight-line segments to produce a conical frustum shape to be used as the nominal center of the free shear layer. Figure 2 sketches this procedure.

Further investigation of the Ref. 5 theory indicated that, for the desired emphasis on the wake relatively close to the body ($x/d \leq 6$), a different procedure would be better. An adequate set of data was located (Refs 6 - 11) to develop correlations for the wake neck location, neck diameter, and downstream (front) shape. Most of these data were obtained in He flows; some were in N_2 flows. No correlations were attempted to account for any effects of such γ variation. The procedure that was used is sketched in Fig. 3. Neck location was estimated using a trend (curve slope) set by cylinder data, applied to one sphere point. Neck diameter was estimated using a related, but multi-step, operation. First, the ratio of sphere-to-cylinder neck diameters was estimated, then this ratio was used to produce the variation of sphere neck diameter with Reynolds number (Re) at one Mach number (M_∞). Next, at a constant value of Re, the variation of sphere wake neck diameter with M_∞ was generated using the trend set by cylinder data and extrapolated to the desired value of M_∞. Finally, the effect of Re was included. Throughout this discussion, the Reynolds number is based on freestream conditions and body diameter.

The wake front downstream of the neck was estimated based on assuming that $y/d = b(x/d)^m$, which is typical of most hypersonic wakes; for instance, see Ref. 5. The exponent value, m, was found to be independent of Re, and insensitive to M_∞ as discussed below. Thus, a "best guess" value was made based primarily on sphere data at $M_\infty = 16$. The scale factor (or intercept) value, b, was based on limited sphere data extrapolated to the desired Re value using the trend set by more extensive cylinder data.

During application of this procedure, several extrapolations in Mach number where necessary. Fortunately, the wake shape is relatively insensitive for $M_\infty \geq \approx 10$, as shown in Fig. 4 and in Ref. 9. Figures 5-8 detail the data and extrapolations actually used, following the steps sketched in Fig. 3. Figure 5 shows the neck location estimation as sketched in Fig. 3a, including the Reynolds number sensitivity shown in Fig. 6. The neck diameter estimation sketched in Fig. 3b is presented in Fig. 7. The results of these two steps indicate the wake neck to be:

$$(x/d)_N = 1.1 \pm .2$$

$$(y/d)_N = 0.2 \pm .1$$

where x = measured from aft end of body

y = measured normal to axis of symmetry

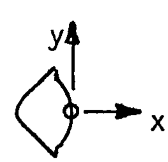

The exponent of the far wake shape, m, was found to be approximately .25 ± .05 as shown in Fig. 8a, from the procedure sketched in Fig. 3c. Similarly the scale factor, b, was approximately .25 ± .05. However, this scale factor cannot be set independently of the above neck location, diameter, and exponent term. That is, for the equation $y/d = b\ (x/d)^m$ with y_N, x_N, and m being given, b is constrained. For this study, individual values of b were computed that would be consistent with the specific neck location and exponent being used. Such values were in general agreement with the limited data shown in Fig. 8b. These relations were transformed to conform with the coordinates used in this study.

Neck Location

$$X/R = 2.8 \pm 0.4 \qquad (1)$$

$$r/R = 0.4 \pm 0.2$$

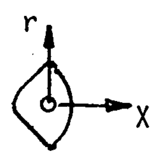

Downstream of Neck

$$r/R = b\ (X/R)^m \qquad (2)$$

$$m = 0.25 \pm 0.05$$

Pressure Boundary

A constant static pressure boundary was used to determine the near viscous wake shear layer edge conditions. To use the constant pressure boundary assumption the base pressure must be known. This work used the data and nominal value extrapolation proposed by Brant and Nestler (Ref. 12) as shown in Fig. 9. Unfortunately, the nominal base pressure correlation when used in the MOC did not yield consistent agreement with neck location correlation developed independently. As a result, several parametric runs were made with the MOC to study the sensitivity of the near wake geometry to the base pressure and forward cone angle.

The effect of cone angle was studied since the wake goemetry correlation had no data for the Jovian probe included in it and the probe geometry was assumed to yield an equivilent wake geometry as a sphere. Moreover, two of the three HYVIS forebody solutions provided for this work were for a 43.5° half-angle hyperboloid which was simulating a hemisphere - 50° cone body. The third solution was for the actual Jovian probe which is a hemisphere - 45° cone body.

The effect of forebody cone angle on the inviscid constant pressure boundary is shown in Fig. 10. As the cone angle decreases, the wake broadens for the range of conditions examined. The reason this occurs can be explained with the aide of the following figure.

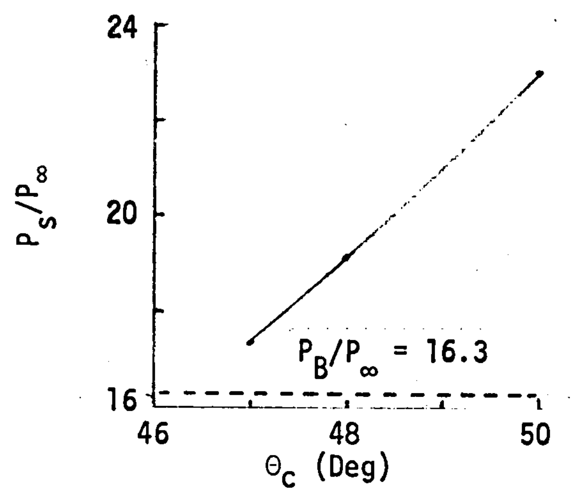

Fig. 11 Shoulder Pressure as a Function of Cone Angle (Case 2)

Figure 11 shows that as the bluntness of the body increases (i.e. increasing Θ_c), the shoulder pressure increases. The base pressure was held constant at $P_B/P_\infty = 16.3$ for all three cone angles. Since the shoulder pressure approaches the base pressure as Θ_c is decreased, the turning angle at the end of the shoulder to achieve the base pressure decreases as Θ_c is decreased. This yields the wake shapes given in Fig. 10.

None of the results shown in Fig. 10 for Case 2 came close to satisfying the wake neck geometry correlation and the trends shown by Fig. 11 indicated that none would be found. Accordingly, the base pressure correlation was examined and modified using a lower base pressure extrapolation as shown in Fig. 9. The resulting wake geometry is shown in Fig. 12. The neck location indicated by the circle for the lower pressure is much closer to the neck location correlation. The same effect was found for Case 3 and consequently the lower pressure extrapolation shown in Fig. 9 was used for Case 3.

After the current model was implemented and flowfield calculations made, some recent data were published on the Jovian probe wake shape. The free flight shadowgraph data reported by Park, Ref. (13), is shown in Fig. 12 for $M_\infty \simeq 16.5$ in an argon/oxygen mixture. The comparison is satisfactory.

2.3 Inviscid Far Wake

The inviscid far wake was calculated using the MOC program using initial conditions from the near wake. The far field inviscid wake started with initial condition from the near wake calculation along the vertical dashed line shown in Fig. 1. The MOC treated the far viscous wake as a solid boundary defined by Eq. (2) from the previous section. The wake shock was calculated as part of the overall MOC solution.

Calculations were made from the wake neck to $X/R \approx 12$. The results were stored on tape for interpolation into cylindrical coordinates. The results along the viscous wall boundary were tabulated and used as edge conditions for the far viscous wake calculation.

2.4 Viscous Near and Far Wake

The near and far viscous wakes were calculated using a modified form of the computer program documented in Ref. (14). The basic features of the program and its current application are described below.

The conservation equations for two dimensional or axisymmetric viscous mixing flow were written in terms of stream functions. An explicit finite difference equation was constructed for the axial momentum equation to evaluate velocity. The axial momentum equation is:

$$\frac{\partial u}{\partial x} = - \frac{1}{\rho u} \frac{dP}{dx} + \frac{1}{\psi^n} \frac{\partial}{\partial \psi} \left(a \frac{\partial u}{\partial \psi} \right) \tag{3}$$

where $a = \mu \rho u y^{2n} / \psi^n$ (4)

and $\psi^n \partial \psi / \partial y = \rho u y^n$ (5)

The term n is o for two-dimensional flow and 1 for axisymmetric flow. The resultant velocity values are applied in a similarity procedure to determine the degree of mixing. The degree of mixing is calculated using

$$F = \frac{U_e - U}{U_e - U_r} \tag{6}$$

In the current application, F represents the fraction of ablation products mixed with the external H_2 and He species.

The temperature of the mixed composition is then determined under the restraint of chemical equilibrium conditions. The velocity, temperature and other properties are located in the physical plane by an inverse transformation from the stream function plane.

The eddy viscosity model used in this study is a Prandtl-like model for compressible flow:

$$\mu = \frac{(\Delta Y + \delta^*_{initial})}{900} \left| (\rho U)_{max} - (\rho U)_{min} \right| + 10^{-4} \tag{7}$$

Other models were used but were found to yield more rapid spreading than the observed viscous wake boundaries would indicate is realistic.

The chemical equilibrium shear layer (CESL) program was used to calculate the near wake and far wake viscous wakes. Both near and far wake calculations required special handling as described below.

The wall enthalpy and pressure at the last station on the cone section of the body were used as special conditions in the near wake calculation. The wall enthalpy and pressure were used as total conditions and with the corresponding elemental composition, expanded isentropically to the base pressure to obtain U_r and related flow parameters. These conditions were used as reference conditions in the shear layer calculation. The velocity profile used is as schematically shown below:

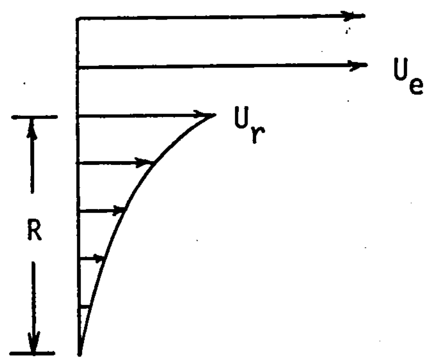

The shape of the profile was changed until the following conditions could be met simultaneously by the dividing streamline.

(1) Total post shock pressure of the dividing streamline matches the static pressure behind the neck shock.

(2) The mass flow rate of the ablation products in the streamlines above the dividing streamline globally matches the ablation mass loss of the forebody predicted by HYVIS.

These two constraints permitted closure of the recirculation zone.

The near wake shear layer was calculated using axisymmetric flow. Since in reality there is a normal component of momentum produced by the external flow, the shear layer necks inward and streamlines converge. To approximate this behavior, the shear layer was transformed along its entire length to conform with the inviscid constant pressure boundary. The results were isentropically compressed at the neck axial station to obtain the initial conditions for the far wake calculation.

The far wake calculations were made with an axial pressure and corresponding edge condition variation predicted by the MOC. These calculations were made with axisymmetric equations of motion and therefore no adjustments were required. In order to make these calculations for variable pressures, the CESL program was modified to handle multiple tables of thermodynamic data at different pressure levels. Moreover, an isentropic type interpolation scheme for evaluating properties between tables was devised and incorporated.

2.5 Recirculation Zone

The recirculation zone analysis was restricted by the near viscous shear layer results. In principle, the flow for streamlines below the dividing streamline should be turned back into the recirculation zone. These streamlines could be mixed to obtain the bulk enthalpy and elemental composition. However, for the Jovian probe case, a limiting condition on the usual precedure was found.

The reference streamline discussed in the previous section had a total pressure greater than the post shock neck static pressure. This implied that the dividing streamline must be less energetic. Viscous disipation is the only mechanism to achieve this lower energetic flow. Since it was not believed possible in a practical sense to obtain a lower energetic flow than the wall condition at the shoulder of the cone, this enthalpy was chosen as the recirculation zone enthalpy. Based on this enthalpy, the base pressure and the elemental composition at the wall the recirculation zone conditions were calculated using chemical equlibrium.

It should be noted, that to the author's knowledge, all previous closure criterion for the recirculation zone have been for low wall enthalpies and small or no ablation product mass flows. The Jovian probe case finds exception to both of these rules.

Table 1

SPECIFYING CONDITIONS

Variable	Case 1	Case 2	Case 3
Time (sec)	109	111	85.25
Altitude (km)	98.29	87.86	93.346
Atmosphere Mass Fractions			
H_2	.641	.641	.641
He	.359	.359	.359
P_∞ (atm)	.003031	.005054	.004429
T_∞ (K)	161.27	156.95	132.07
M_∞	43.946	38.466	46.975
V_∞ (m/sec)	38969	33649	37547

Table 2a

Case 1
COMPARISON OF EQUILIBRIUM
THERMODYNAMIC CALCULATIONS

Variable	Condition 1		Condition 2		Condition 3	
	REMTECH	Langley	REMTECH	Langley	REMTECH	Langley
P atm	7.622	7.622	4.642	4.642	4.566	4.566
T K	16998	16998	13730	13730	4215	4215
H cal/gm	179381	179323	110377	110317	6219.7	6203.6
$\bar{M}$ Mol wt	1.075	1.075	1.254	1.254	27.969	28.045
c_p cal/gm K	29.9569	-----	18.3626	-----	2.8705	-----
γ	1.2192	-----	1.2207	-----	1.1130	-----
a m/sec	12660.3	-----	10541.0	-----	1180.9	-----
Mole Fractions						
H	.46374	.46382	.70739	.70754	.16378	.16246
H_2	.00001	.00001	.00004	.00004	.02398	.024015
H^+	.21986	.21990	.09004	.09006	-----	-----
He	.09631	.09615	.11248	.11230	.00126	.00126
He^+	.00011	.00011	.00001	.00001	-----	-----
e-	.21997	.22001	.09005	.09000	-----	-----
C	-----	-----	-----	-----	.02788	.02739
C_2	-----	-----	-----	-----	.02821	.02785
C_3	-----	-----	-----	-----	.30748	.30655
C_2H	-----	-----	-----	-----	.11369	.11384
C_2H_2	-----	-----	-----	-----	.00923	.00933
C_3H	-----	-----	-----	-----	.09487	.09570
C_4H	-----	-----	-----	-----	.12480	.12647
CO	-----	-----	-----	-----	.10483	.10514

Condition

1 - Post Shock (Stagnation Point)
2 - Post Shock (Station 15)
3 - Wall (Station 15)

Table 2b

Case 2

COMPARISON OF EQUILIBRIUM THERMODYNAMIC CALCULATIONS

	Condition 1		Condition 2	
Variable	REMTECH	Langley	REMTECH	Langley
P atm	9.6279	9.6279	5.6632	5.6632
T K	15469.4	15469.4	11379.4	11379.4
H cal/gm	133261	133222	79022	79000
$\bar{M}$ Mol wt	1.199	1.199	1.349	1.349
c_p cal/gm K	21.721	-----	8.2632	-----
γ	1.2196	-----	1.3085	-----
a m/sec	11437.3	-----	9580.6	-----
Mole Fractions				
H	.63257	.63274	.83593	.83612
H_2	.00004	.00004	.00016	.00016
H^+	.12991	.12992	.02147	.02147
He	.10753	.10735	.12097	.12078
He^+	.00002	.00002	.00000	.00000
e-	.12993	.12995	.02147	.02147
C	-----	-----	-----	-----
C_2	-----	-----	-----	-----
C_3	-----	-----	-----	-----
C_2H	-----	-----	-----	-----
C_2H_2	-----	-----	-----	-----
C_3H	-----	-----	-----	-----
C_4H	-----	-----	-----	-----
CO	-----	-----	-----	-----

Condition
1 - Post Shock (Stagnation Point)
2 - Post Shock (Station 15)

Table 2c

Case 3
COMPARISON OF EQUILIBRIUM
THERMODYNAMIC CALCULATIONS

	Condition 1		Condition 2		Condition 3	
Variable	REMTECH	Langley	REMTECH	Langley	REMTECH	Langley
P atm	12.651	12.651	7.1249	7.1249	7.436	7.436
T K	17125	17125	12999	12999	3978	3978
H cal/gm	166386.	166322.	94742	94716	5417.9	5423.9
$\bar{M}$ Mol wt	1.118	1.118	1.307	1.307	30.824	30.787
c_p cal/gm K	26.2726	-----	12.7979	-----	2.1459	------
γ	1.2215	-----	1.2480	-----	1.1076	------
a m/sec	12474.3	-----	10158.7	-----	1090.1	------
Mole Fractions						
H	.52184	.52199	.77931	.77949	.10850	.10904
H_2	.00003	.00003	.00010	.00009	.03768	.03768
H^+	.18890	.18890	.05168	.05169	------	------
He	.10016	.09999	.11723	.11704	.01757	.01752
He^+	.00009	.00009	------	------	------	------
e-	.18899	.18899	.05168	.05169	------	------
C	------	------	------	------	.00788	.00797
C_2	------	------	------	------	.01026	.01035
C_3	------	------	------	------	.17830	.17900
C_2H	------	------	------	------	.12088	.12101
C_2H_2	------	------	------	------	.02347	.02337
C_3H	------	------	------	------	.14328	.14295
C_4H	------	------	------	------	.23732	.23634
CO	------	------	------	------	.11486	.11474

Condition

1 - Post Shock (Stagnation Point)
2 - Post Shock (Station 17)
3 - Wall (Station 17)

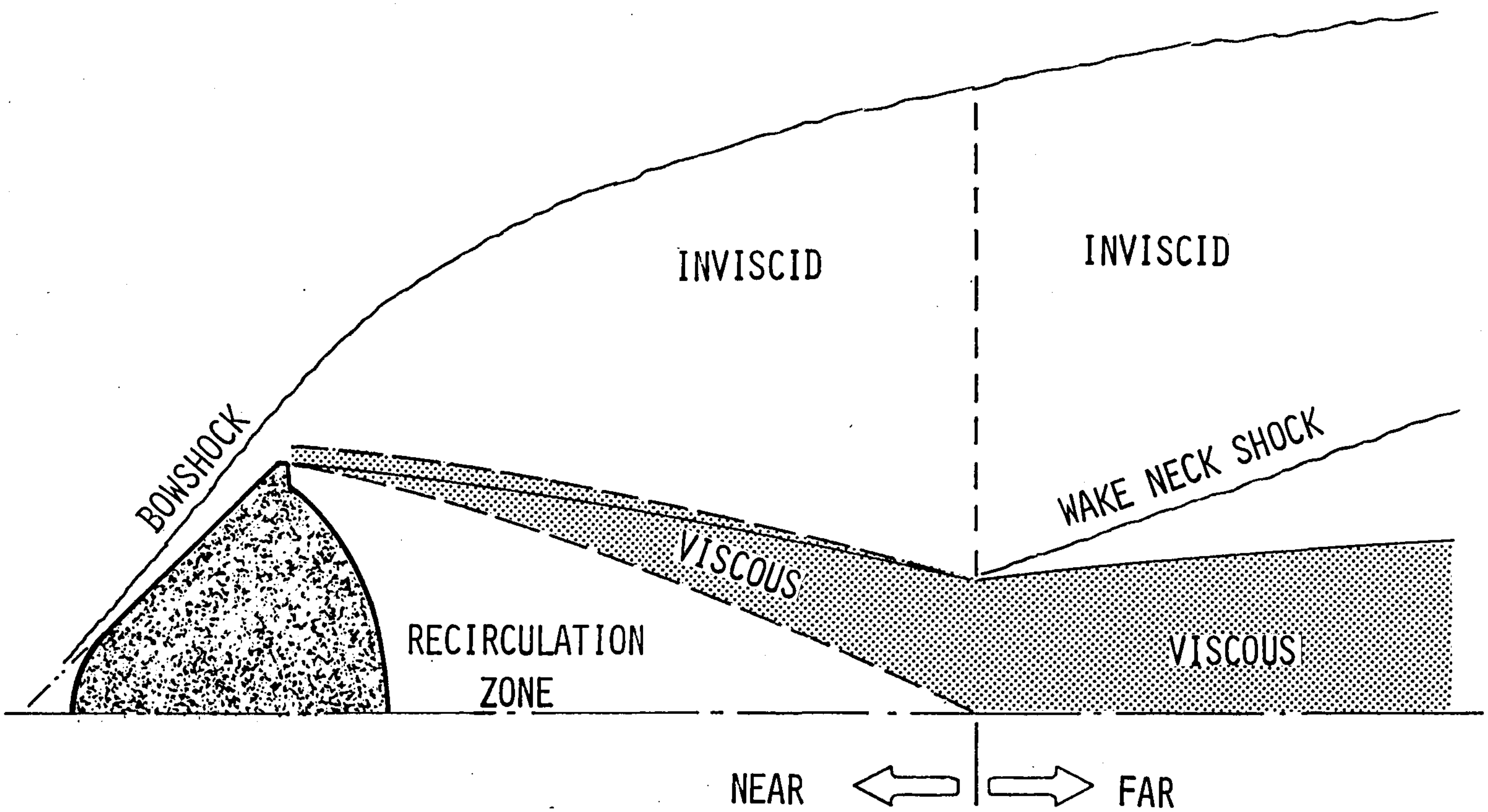

Fig. 1 Computational Regions for the Jovian Probe Wake Flowfield

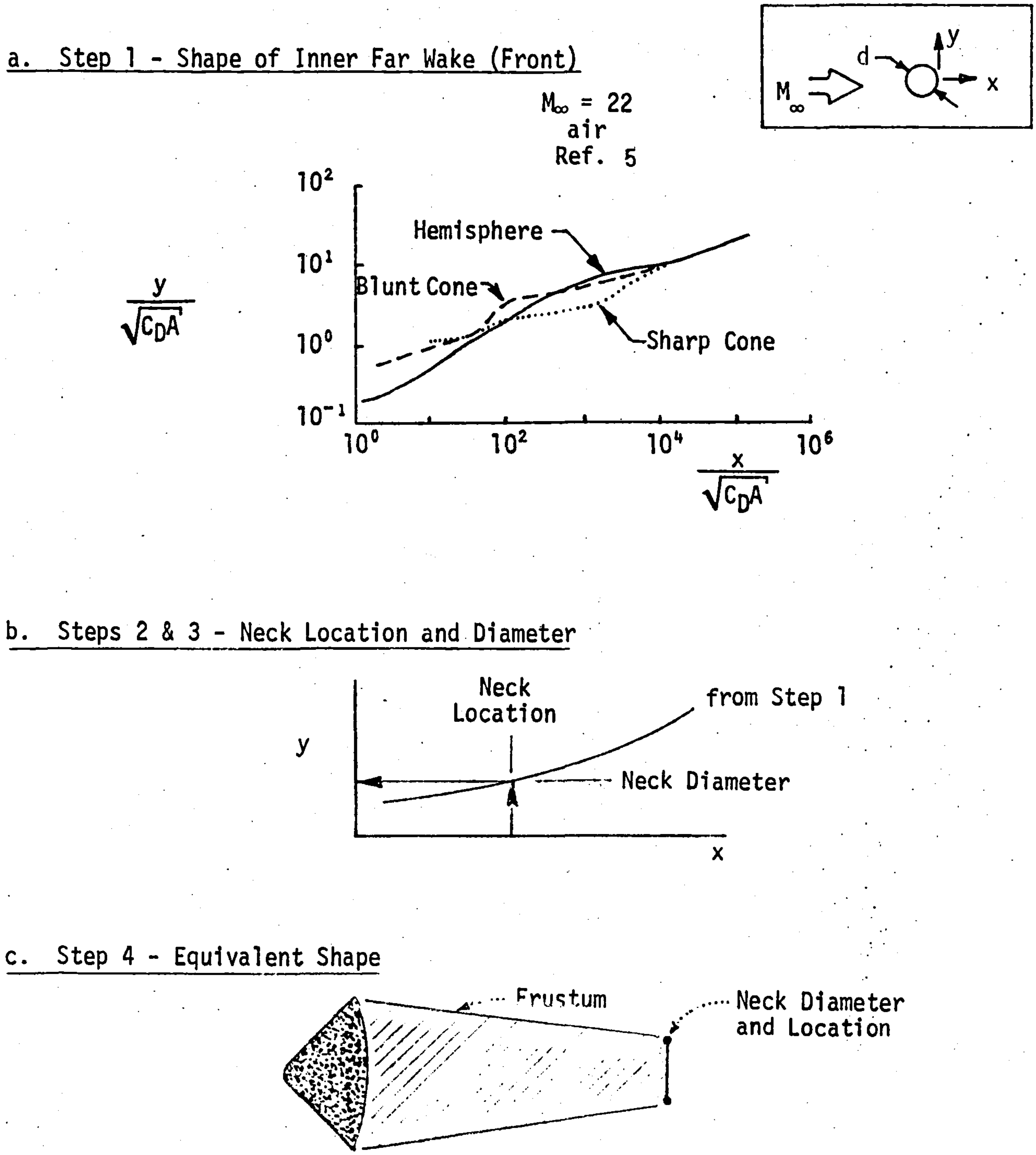

Fig. 2 Schematic of Initially Planned Wake Shape Procedure

a. Neck Location

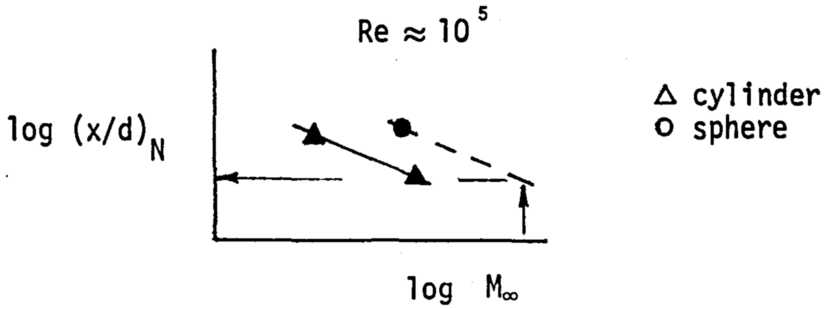

b. Neck Diameter

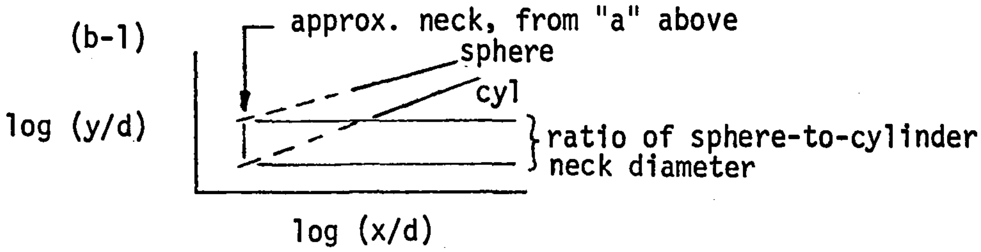

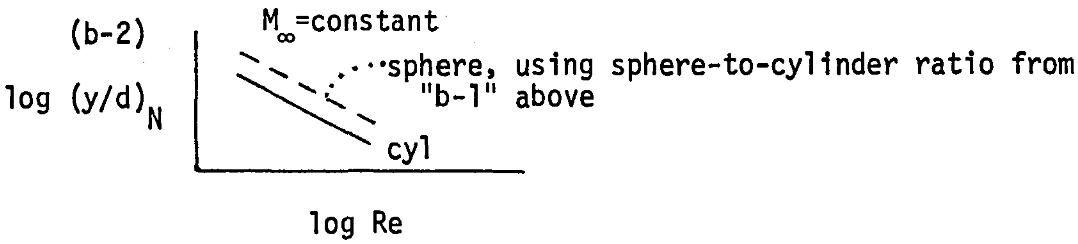

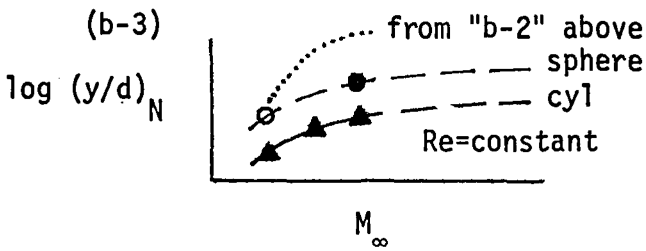

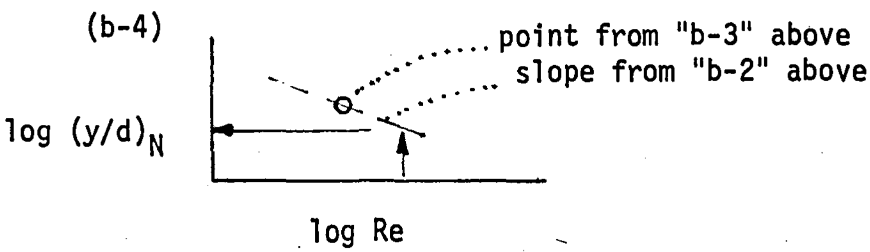

Fig. 3 Schematic of Wake Shape Procedure Used

c. Wake Front Downstream of Neck

Assuming $y/d = b(x/d)^m$

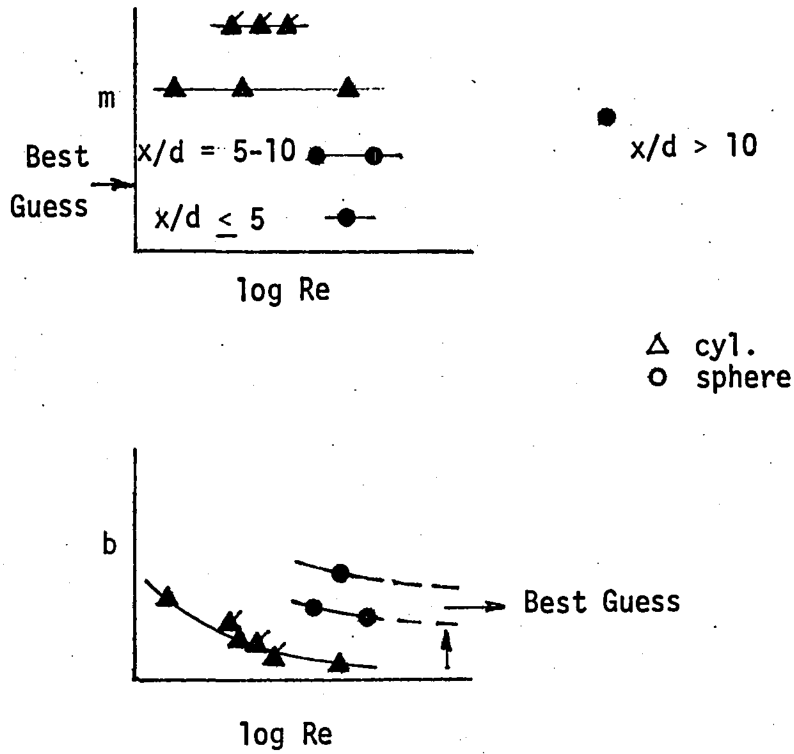

Figure 3 (Concluded).

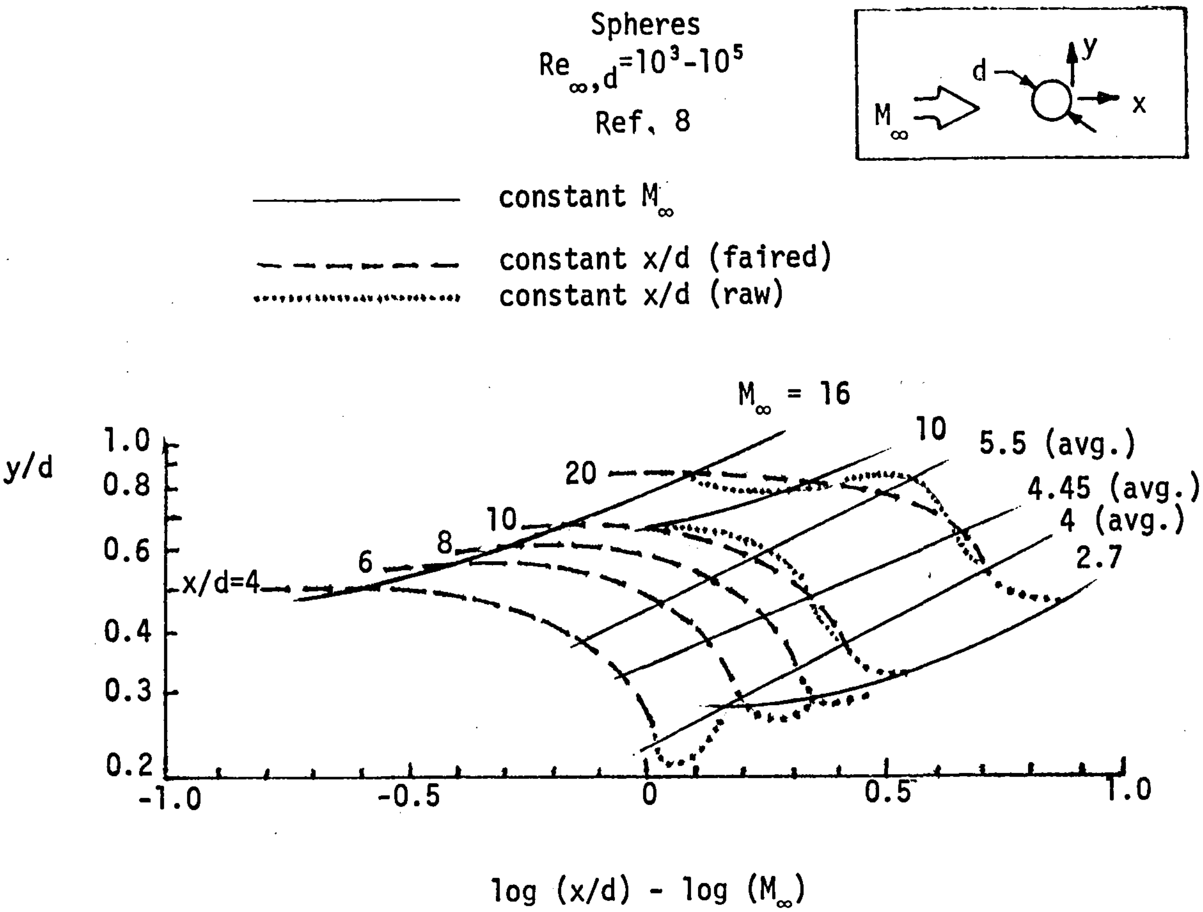

Fig. 4 M_∞ Effect on Wake

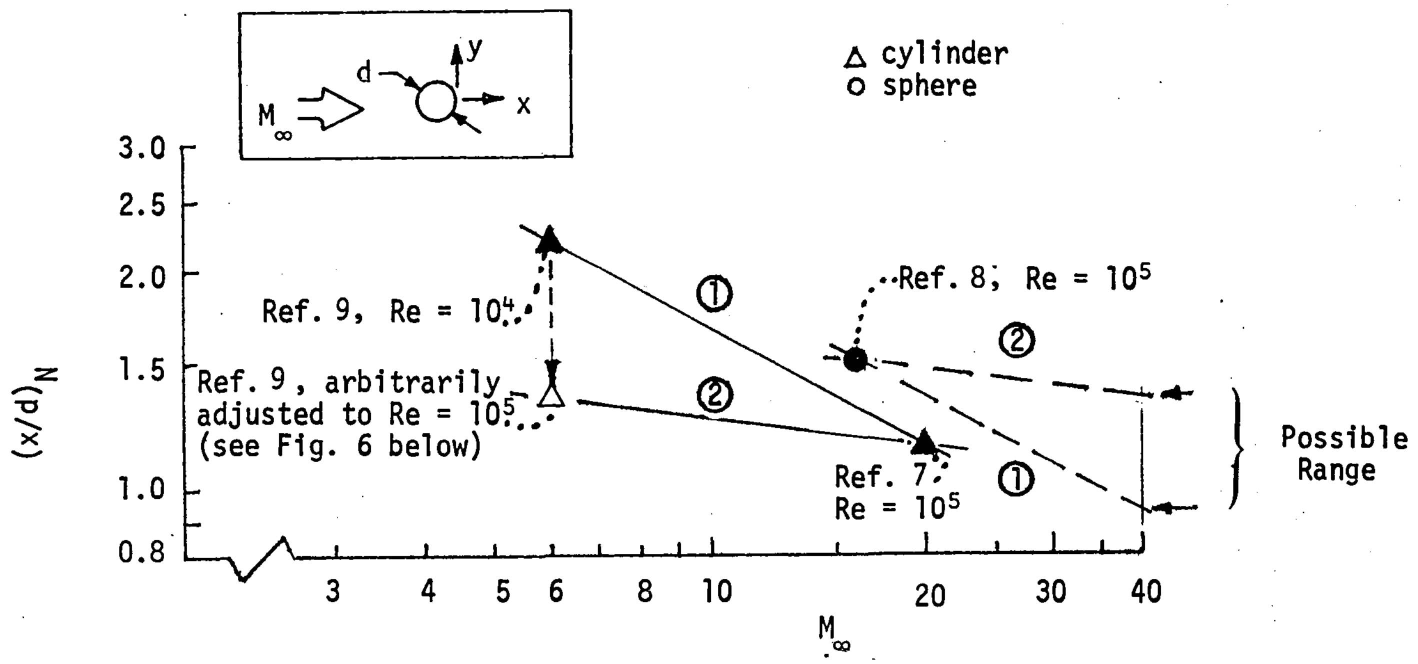

Fig. 5 Neck Location

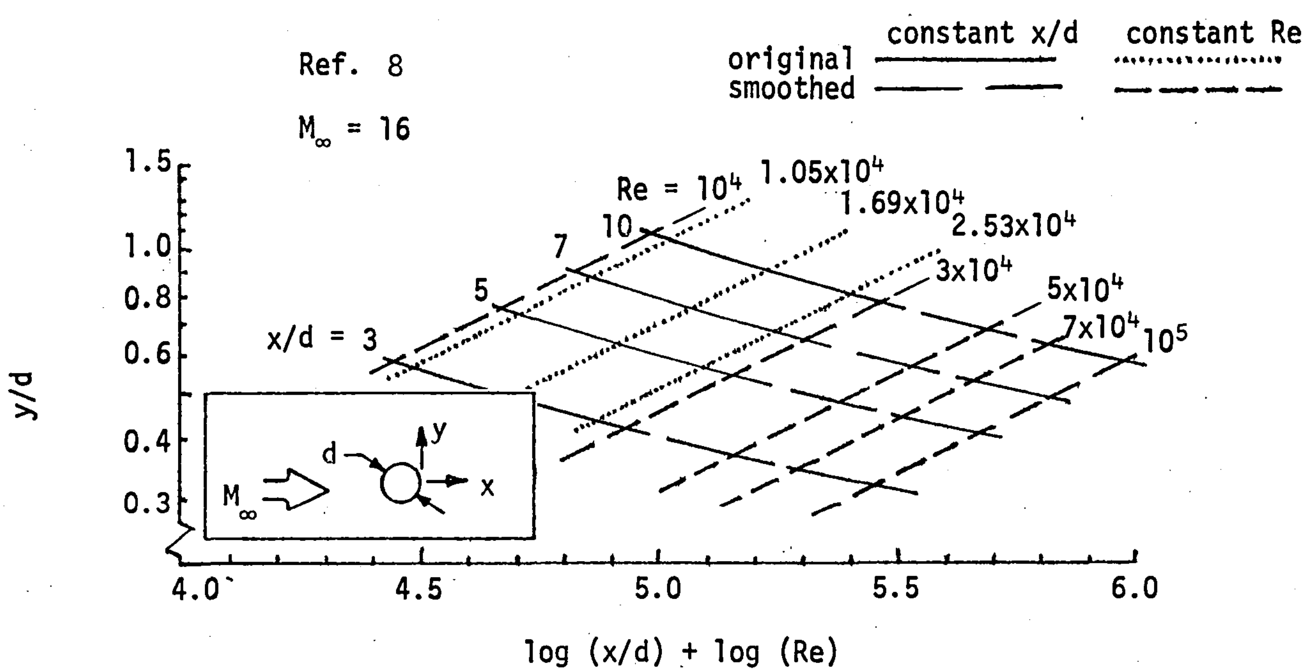

Fig. 6 Reynolds Number Effect on Wake Neck

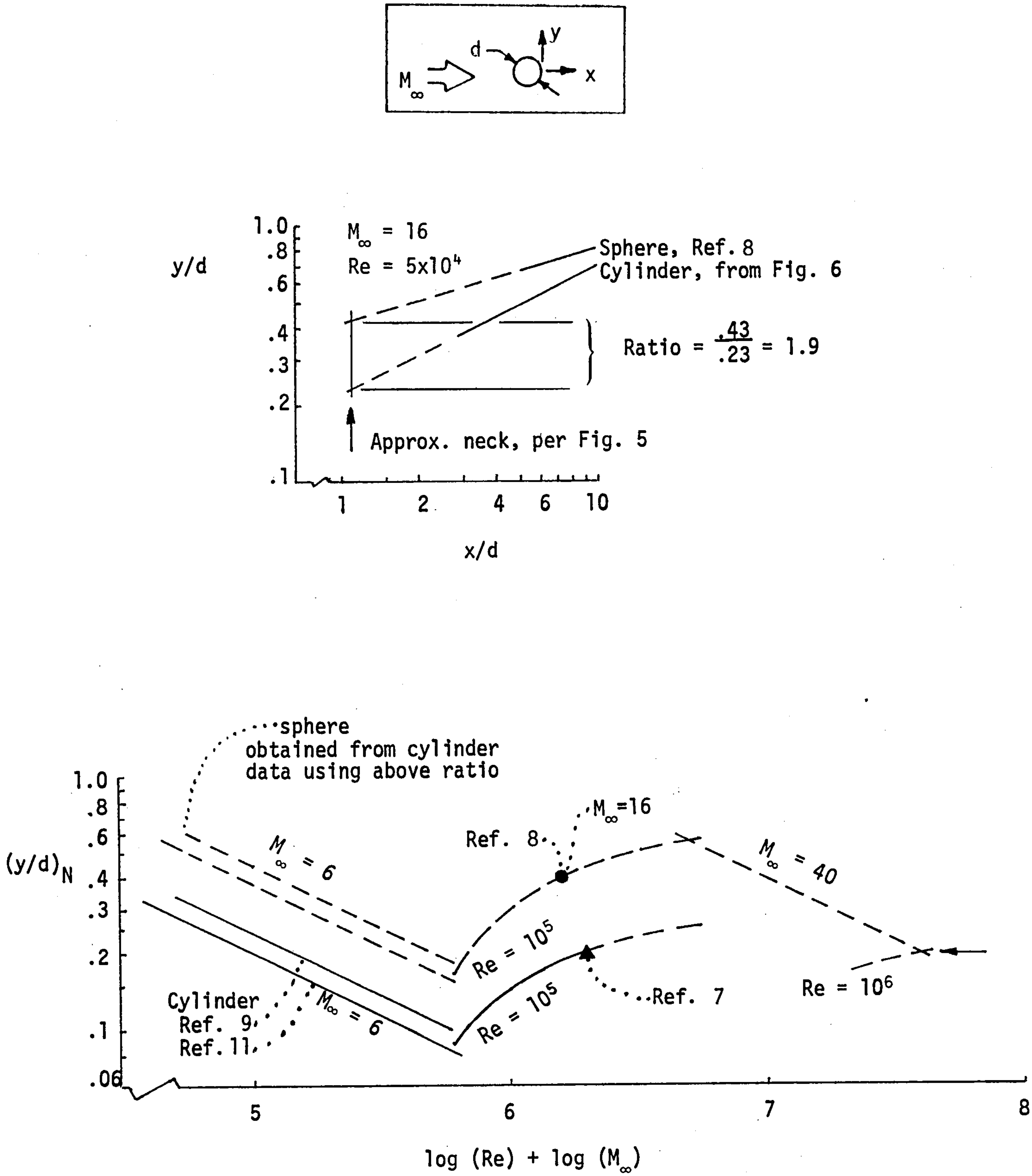

Fig. 7 Neck Diameter

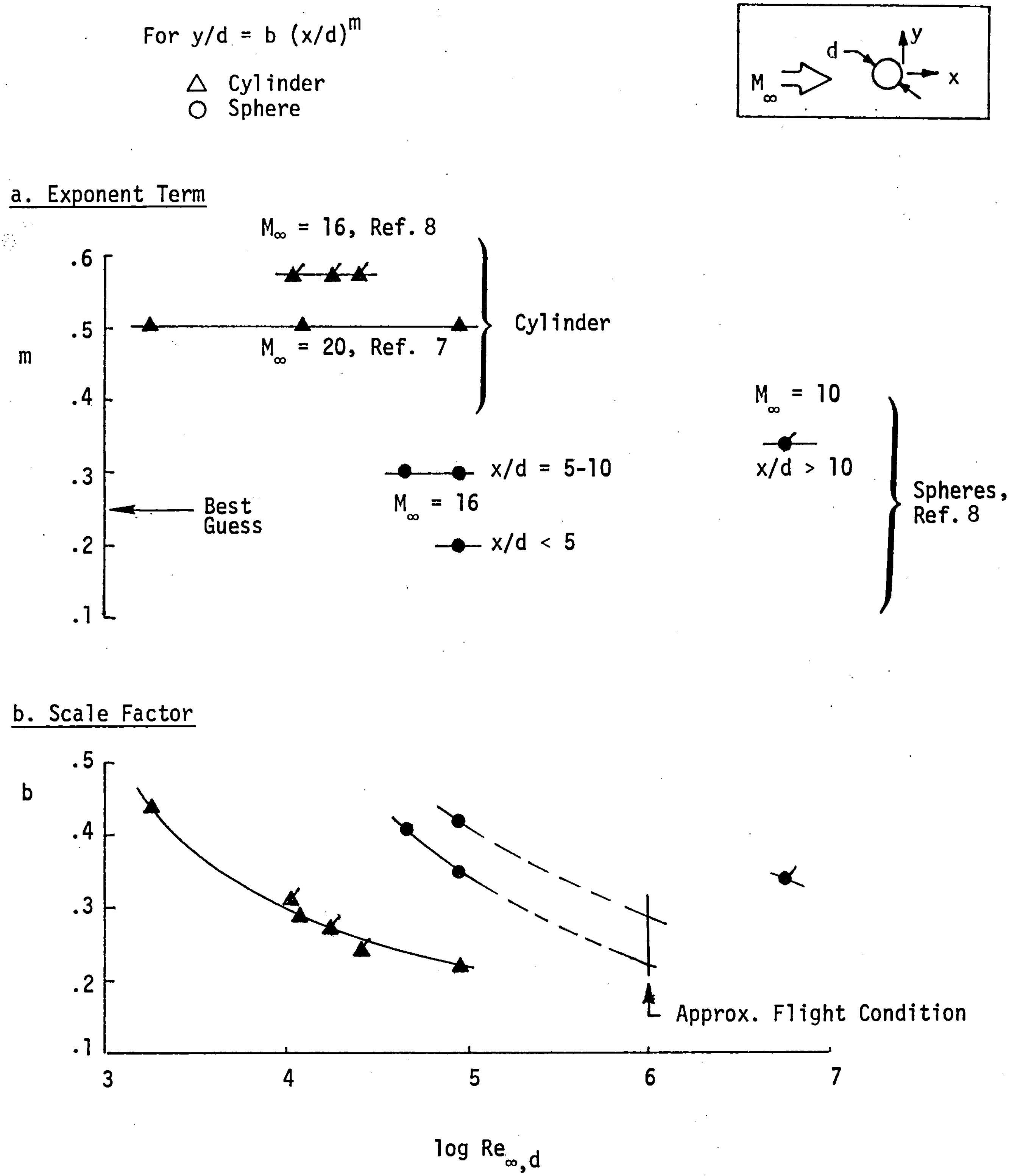

Fig. 8 Wake Front Downstream of Neck

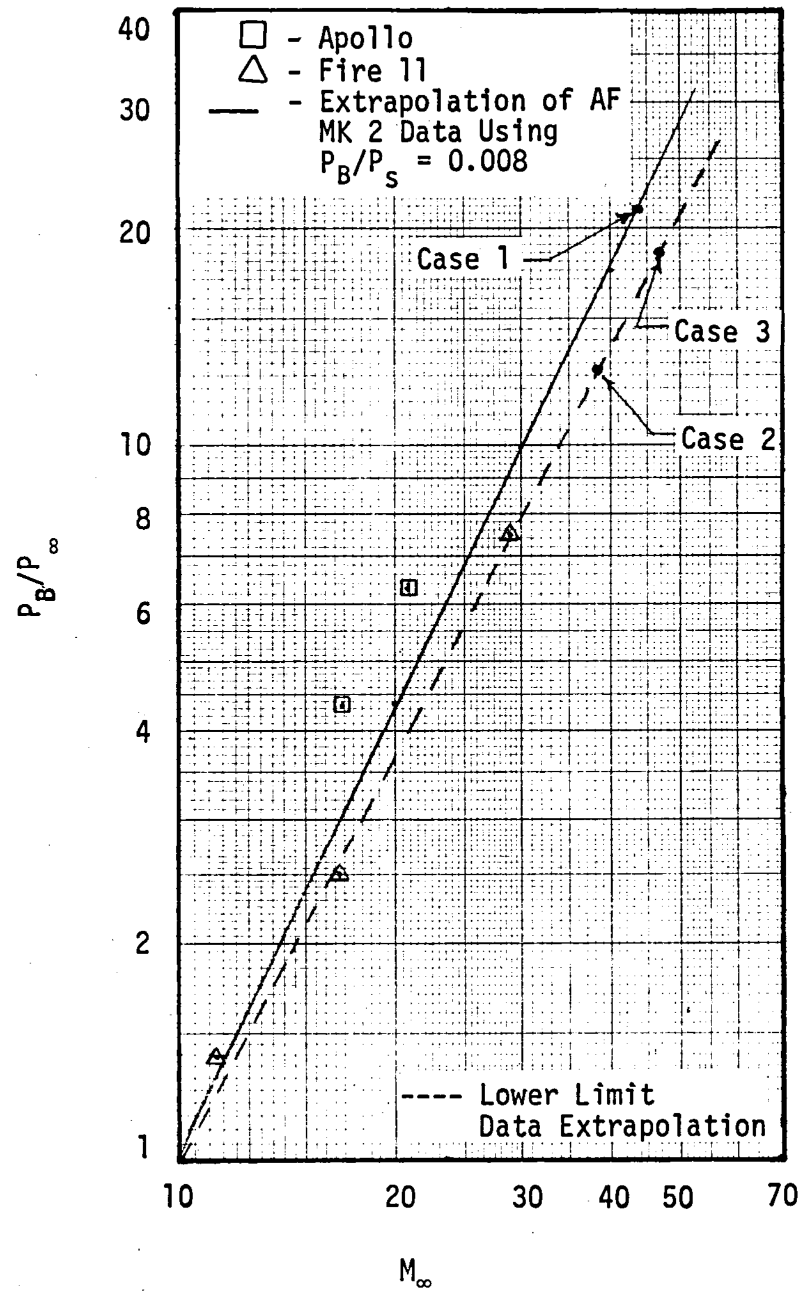

Fig. 9 Turbulent Base Pressure Correlation for Planetary Entry Systems (From Brant and Nestler, Ref. 12)

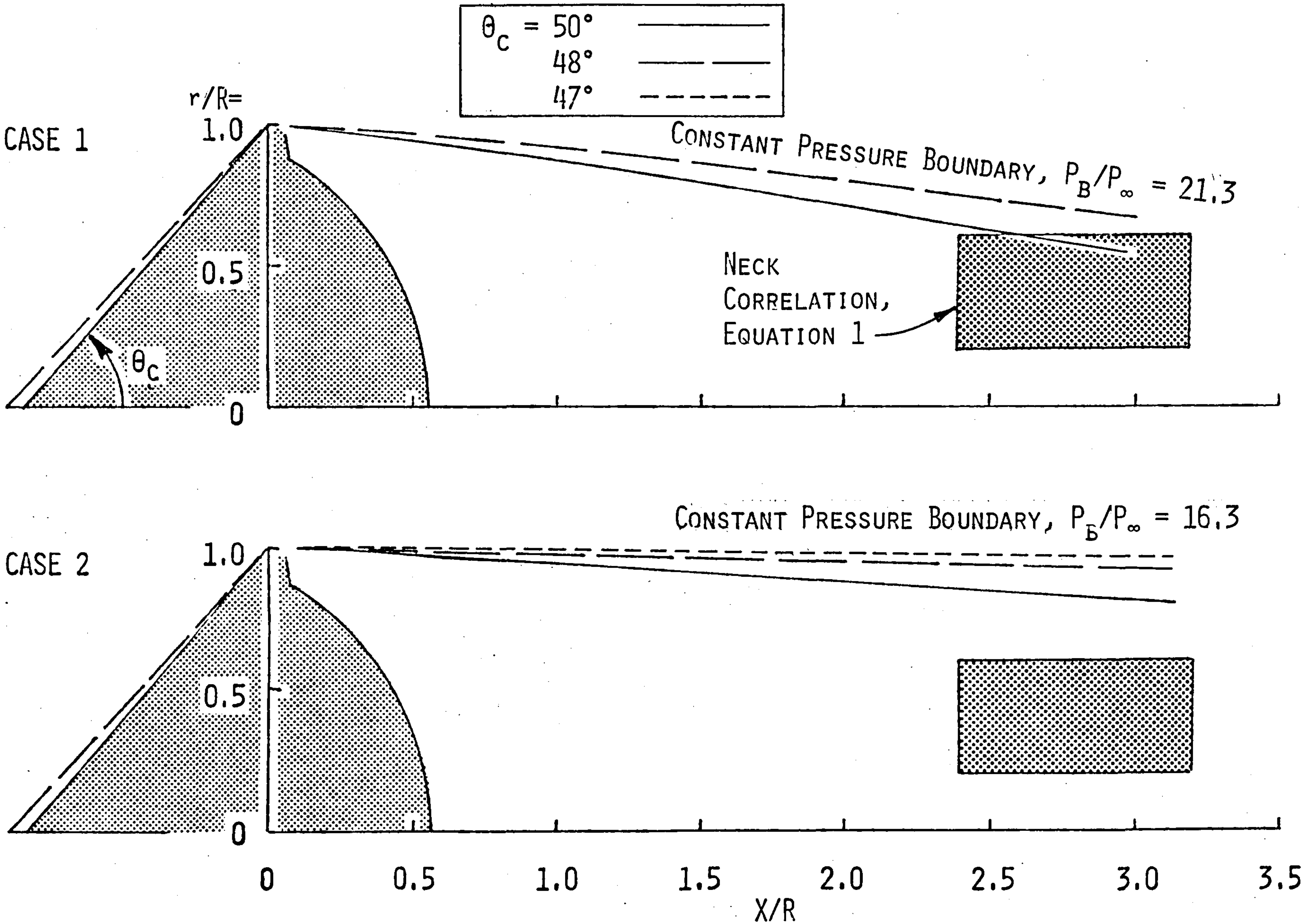

Fig. 10 Effect of Forebody Cone Angle on Inviscid Constant Pressure Boundary

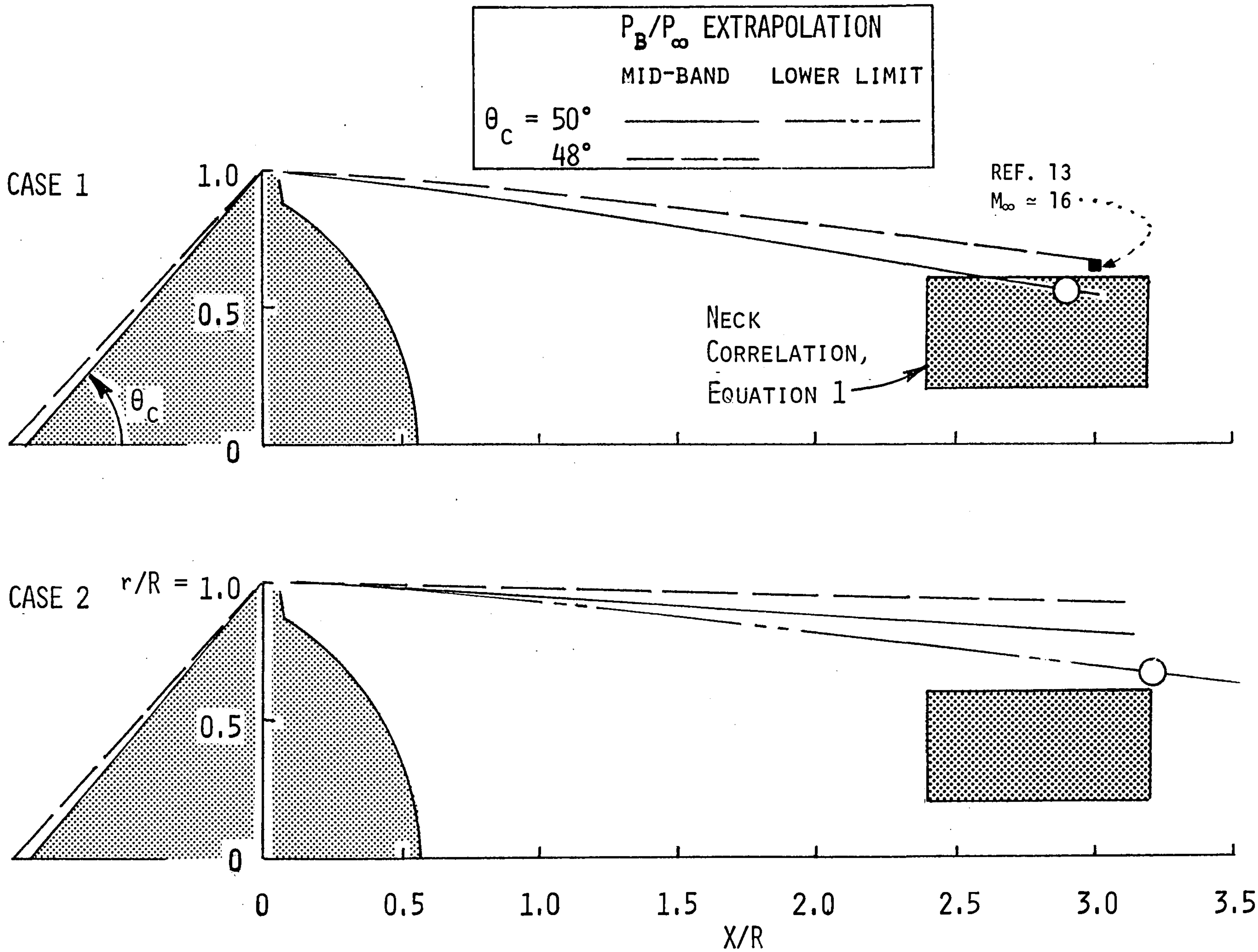

Fig. 12 Effect of Forebody Angle and Pressure Correlation In Near Wake Shape

Section 3.0
RESULTS

This section presents observations about the three wake flowfields calculated and presents the manner in which the flowfields were recorded on tape for radiation analysis work.

3.1 Flowfield Distributions

The analytical methods described in Section 2.0 were used to calculate three flowfields. The specifying conditions for the three cases are given in Table 1.

The starting location for the current flowfields is where the HYVIS program terminates at the end of the Jovian probe conical section. It is therefore appropriate to compare the MOC solution on the conical section with the HYVIS results. Post shock results are given in Table 3 and are found to be in reasonable agreement. Case 3 is in best agreement and both analyses used conic sections for the body. For Cases 1 and 2, the HYVIS program used a hyperboloid. The body angle used in the MOC calculation was larger than the actual body angle to account for effective body displacement due to massive blowing.

Near wake inviscid boundary results for Case 1 are given in Figs. 13 to 15. Figure 13 shows the main shock location and inviscid constant pressure boundary location. The post shock Mach number, temperature, entropy and flow angle are given in Fig. 14. The post shock conditions are constant out to r/R = 1.3 where the expansion fan from the shoulder hits the shock. Beyond r/R = 1.3 the entropy monotonically decreases, resulting in an increase in Mach number and decrease in temperature and flow angle. The radial distributions at the neck axial position are the starting conditions for the far wake solution. These conditions are given in Fig. 15. Note an inflection in Mach number and temperature occurs near r/R = 1.3 and the Mach number is much larger beyond r/R = 2.0 than below 2.0. Correspondingly, the temperature drops significantly beyond r/R = 2.0.

An overall comparison of the inviscid flowfield properties for Cases 1, 2 and 3 is given in Fig. 16. Case 1 has the highest temperatures and pressure ratios and Case 2 exhibits the least severe conditions. The wake neck is the smallest for Case 1 producing the largest turning angle for the flow at the neck. This results in the strongest wake shock and correspondingly highest post shock conditions. Case 3 has the largest viscous wake of the three cases.

Near and far radial temperature profiles are given in Fig. 17 and 18 respectively for several axial positions. The temperature is seen to be constant in the recirculation zone, decrease slightly in the inner part of the shear layer, and then increases to meet the inviscid flow temperature. The temperature distributions in the inviscid flow are not monotonic functions but form consistent trends reflecting both real gas and reflected expansion wave effects. Case 2 shows a rather benign far field from a radiation viewpoint. The near wake specific heat ratio radial distributions are shown in Fig. 19 for four axial positions. Notice that some of the radial distributions exhibit a double peak in gamma and the distribution values vary widely in magnitude. To help explain the process controlling this gamma variation Fig. 20 was prepared. Figure 20 presents the gamma variation as a function of static pressure for specified total pressures. Points A, B, C and D from Fig. 19 at X/R = 1.0 are plotted on Fig. 20. The static pressure increases in the radial direction as well as the total pressure. This combination, as shown in Fig. 20, produces the double peak which appears in the flowfield.

Typical mole fraction distributions in the radial direction are given in Figs. 21 and 22 for the near and far wake respectively of Case 3. The near inviscid wake primarily consists of H and He atoms. Molecules of H_2 start appearing in the far inviscid wake. The C_3 molecule is the most dominant ablation species in the near viscous wake whereas C_4H, C_3H, CO, as well as C_3 are the most dominant species in the far viscous wake.

3.2 Flowfield Tapes

The flowfield results for all three cases were put on tape and delivered to Langley. The flowfield properties are listed in nondimensional cylinderical coordinates starting at the probe shoulder and going to X/R = 10.

The card image format of the tape is given in Table 4. The following description defines the tape type.

9 track	Block size 4800 characters
1600 BPI	3 files, no labels
Odd parity	Record size 80 characters

ANSI interchange format

Each file is written as an ASCII character string with one record being one card image. Files are separated by hardware end-of-file marks, with two marks ending the third file. A copy of the tape creating program written in ANSI Cobol is given in Table 5 and a tape read program written in Fortran is given in Table 6.

Table 3

COMPARISON OF CONE SECTION
POST-SHOCK CONDITIONS

Variable	Units	Case 1		Case 2		Case 3	
		REMTECH	Langley Sta. 15	REMTECH	Langley Sta. 15	REMTECH	Langley Sta. 17
T	K	14,137	13,730	12,285	11,379	13,044	12,999
P	atm	4.891	4.642	6.297	5.663	7.241	7.125
Avg. Mol. Weight	-	1.2338	1.254	1.3277	1.3491	1.3061	1.3074
Θ_s-Θ_c (Blowing)	deg.	4.38	4.81	4.76	3.53	3.91	4.18
Θ_c	deg.	50	47	50	74	46	45

Table 4

CARD IMAGE FORMAT

Card Type	Column	Format	Variable	Definition
1	1 - 80	8A1	TITLE	Title
2	1 - 10	F10.5	X/R	Axial Distance
	11 - 20	F10.5	r/R	Radial Distance
	21 - 30	F10.5	M	Mach Number
	31 - 40	F10.5	Θ	Flow Angle (Deg.)
	41 - 50	F10.5	$\overline{M}$	Molecular Weight
	51 - 60	F10.5	γ	Specific Heat Ratio
	61 - 68	F8.2	T	Temperature (°K)
	69 - 78	F10.5	P	Pressure (atm)
	79 - 80	I2	IS	Number of Species on Following Cards for This Location
3	1 - 4	A4	SN	Species Name
	5 - 10	F6.5	Y_1	Mole Fraction of Species 1
		(repeated)	Y_2	
		8(A4,F6.5)	Y_i	i = 1, IS

Table 5

COBOL TAPE GENERATION PROGRAM

```
@COB,IS ONE,ONE
        IDENTIFICATION DIVISION.
        PROGRAM-ID. F-FORMAT.
        ENVIRONMENT DIVISION.
        CONFIGURATION SECTION.
        SOURCE-COMPUTER. UNIVAC-1100.
        OBJECT-COMPUTER. UNIVAC-1100.
        INPUT-OUTPUT SECTION.
        FILE-CONTROL.
            SELECT TAPE-OUT ASSIGN TO INTERCHANGE T8.
            SELECT IN-REC ASSIGN TO CARD-READER.
        DATA DIVISION.
        FILE SECTION.
        FD  IN-REC
            LABEL RECORDS ARE OMITTED.
         01 PRT-REC                                  PIC X(80).
        FD  TAPE-OUT
            LABEL RECORDS ARE STANDARD
            BLOCK CONTAINS 60 RECORDS
            RECORDING MODE IS F .
        01  REC-IN.
            02 B                                       PIC X(80).
        WORKING-STORAGE SECTION.
        77  CTR VALUE 0                                PIC 9(5).
        77  CTR1 VALUE 0                                PIC 9(5).
        77  NUMBER-RECS-PROCESSED                      PIC ZZ,ZZ9.
        PROCEDURE DIVISION.
        HOUSE-KEEPING.
            OPEN INPUT IN-REC.
            OPEN OUTPUT TAPE-OUT WITH NO REWIND.
        INFINITE-LOOP.
            READ IN-REC
               AT END GO TO END-OF-JOB.
            WRITE REC-IN FROM PRT-REC.
            ADD 1 TO CTR ON SIZE ERROR
               DISPLAY 'ADD 99,999 TO RECS PROCESSED' UPON
                  PRINTER MOVE 1 TO CTR.
            GO TO INFINITE-LOOP.
        END-OF-JOB.
            CLOSE TAPE-OUT WITH NO REWIND.
            MOVE CTR TO NUMBER-RECS-PROCESSED.
            DISPLAY 'NUMBER OF RECS PROCESSED  '
               NUMBER-RECS-PROCESSED UPON PRINTER.
            CLOSE IN-REC.
            STOP RUN.
```

Table 6

FORTRAN TAPE READ PROGRAM

```
000     @FOR,IS MAIN,MAIN
000     C      THIS PROGRAM READS AN ANSI INTERCHANGE TAPE
000     C      THE INTERCHANGE FORMAT IS SET BY THE FOLLOWING 'DEFINE FILE'
000     C      STATEMENT.
000     C      ANSI = SET ANSI INTERCHANGE - NO USER LABELS.
000     C      FB = FIXED BLOCK LENGTH.
000     C      80 = 80 CHARACTERS PER RECORD.
000     C      4800 = 4800 CHARACTERS PER BLOCK.
000     C
000     C      THIS PROGRAM ASSUMES 3 TAPE FILES SEPARATED BY END-OF-FILE MARKS.
000     C
000             DEFINE FILE 8(ANSI,FB,80,4800)
000             DIMENSION I(20)
000             N=0
000       8     N=N+1
000             IF (N.EQ.4) GO TO 999
000            PRINT 400, N
000            DO 20 J=1,50
000             READ(8,100) I
000             PRINT 300,I
000      20     CONTINUE
000             DO 50   J=1,5000
000      50      READ(8,100,END=8) I
000     100 FORMAT(20A4)
000    300  FORMAT (1H ,20A4)
000     400 FORMAT(1H1,'FILE',I2,'    FIRST 50 RECORDS',/)
000    999    STOP
000           END
```

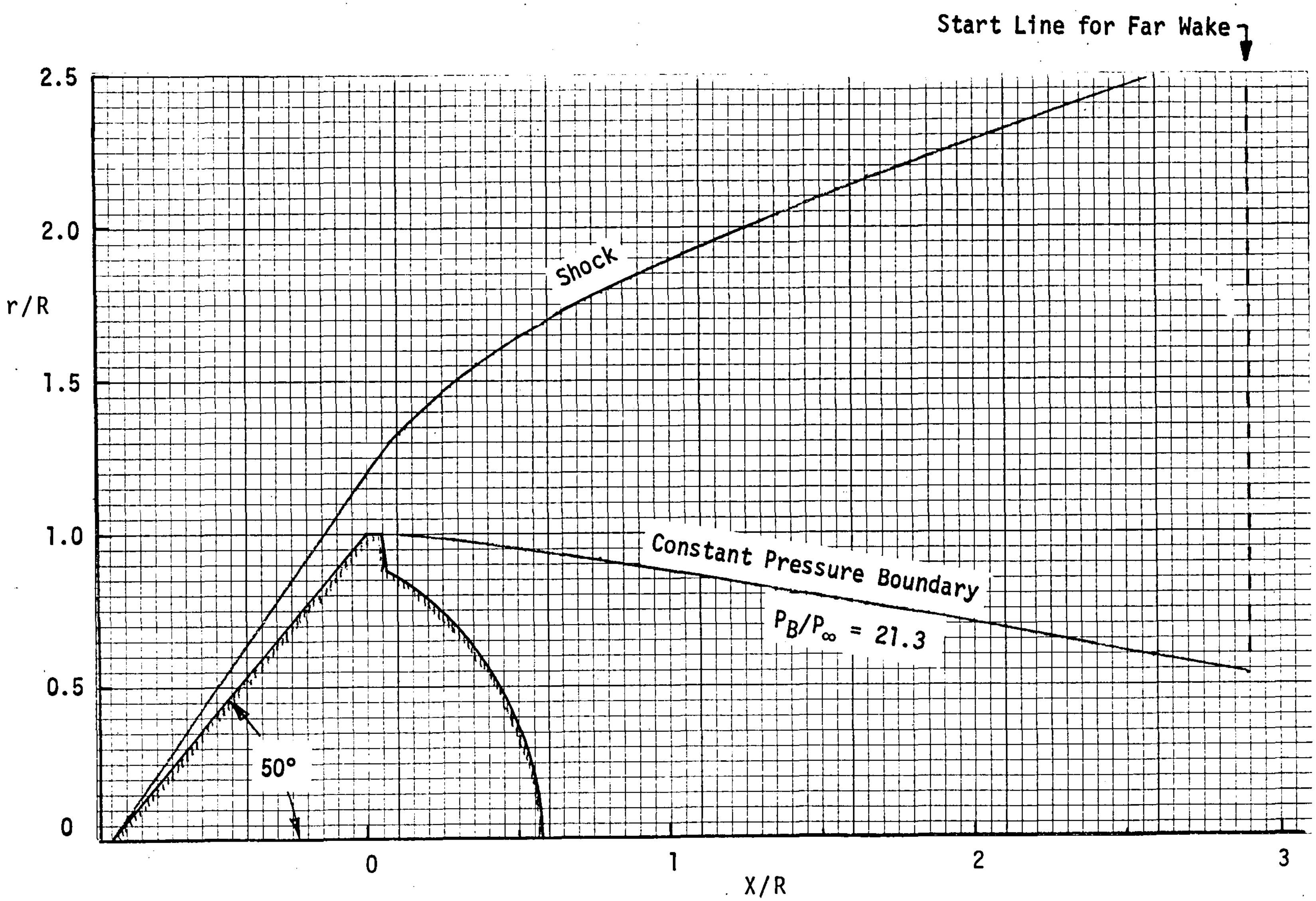

Fig. 13 Shock and Inviscid Constant Pressure Boundary for the Near Wake (Case 1 Final)

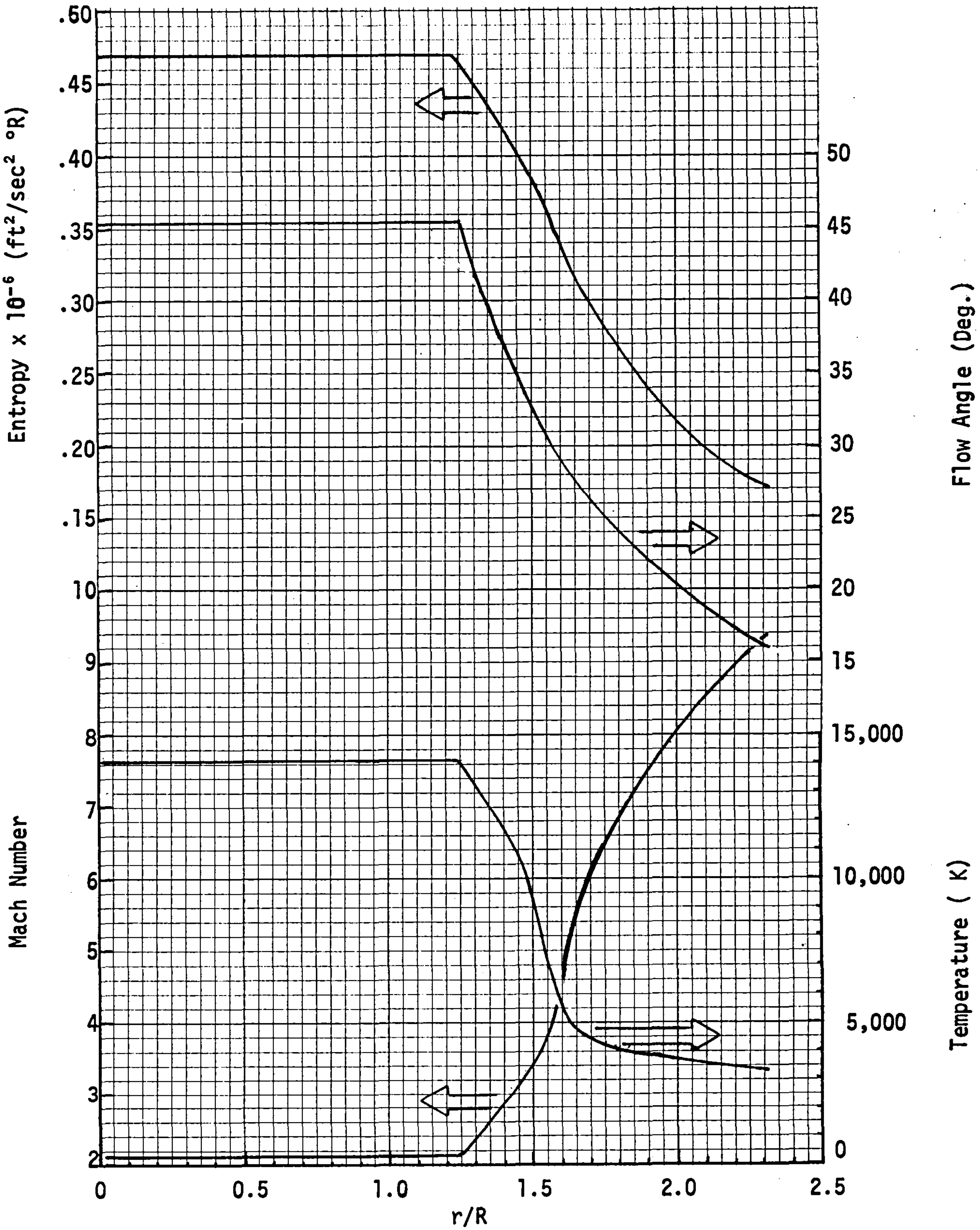

Fig. 14 Post-Shock Properties (Case 1 Final)

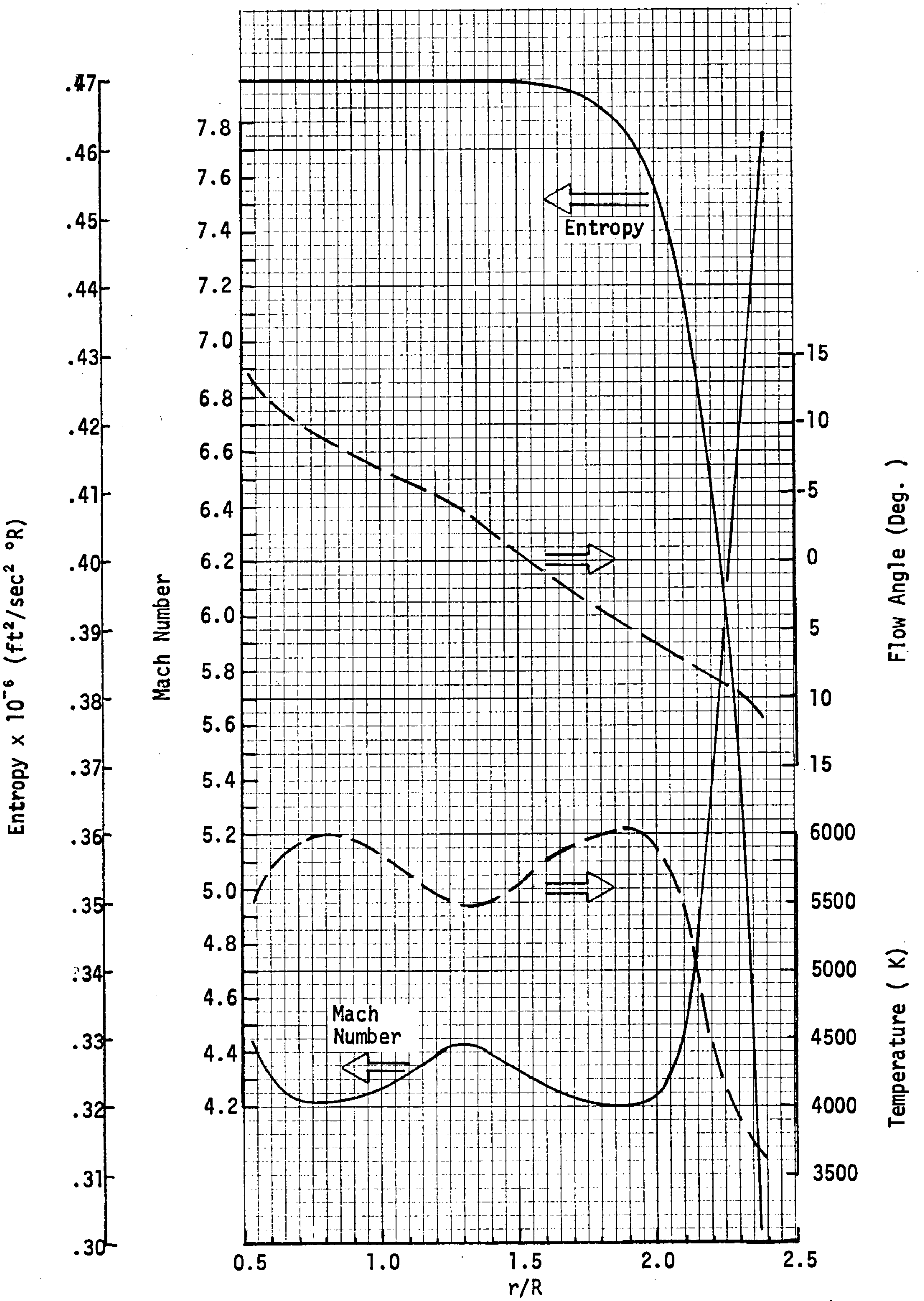

Fig. 15 Start Line Properties for Far Wake at X/R=2.9 (Case 1 Final)

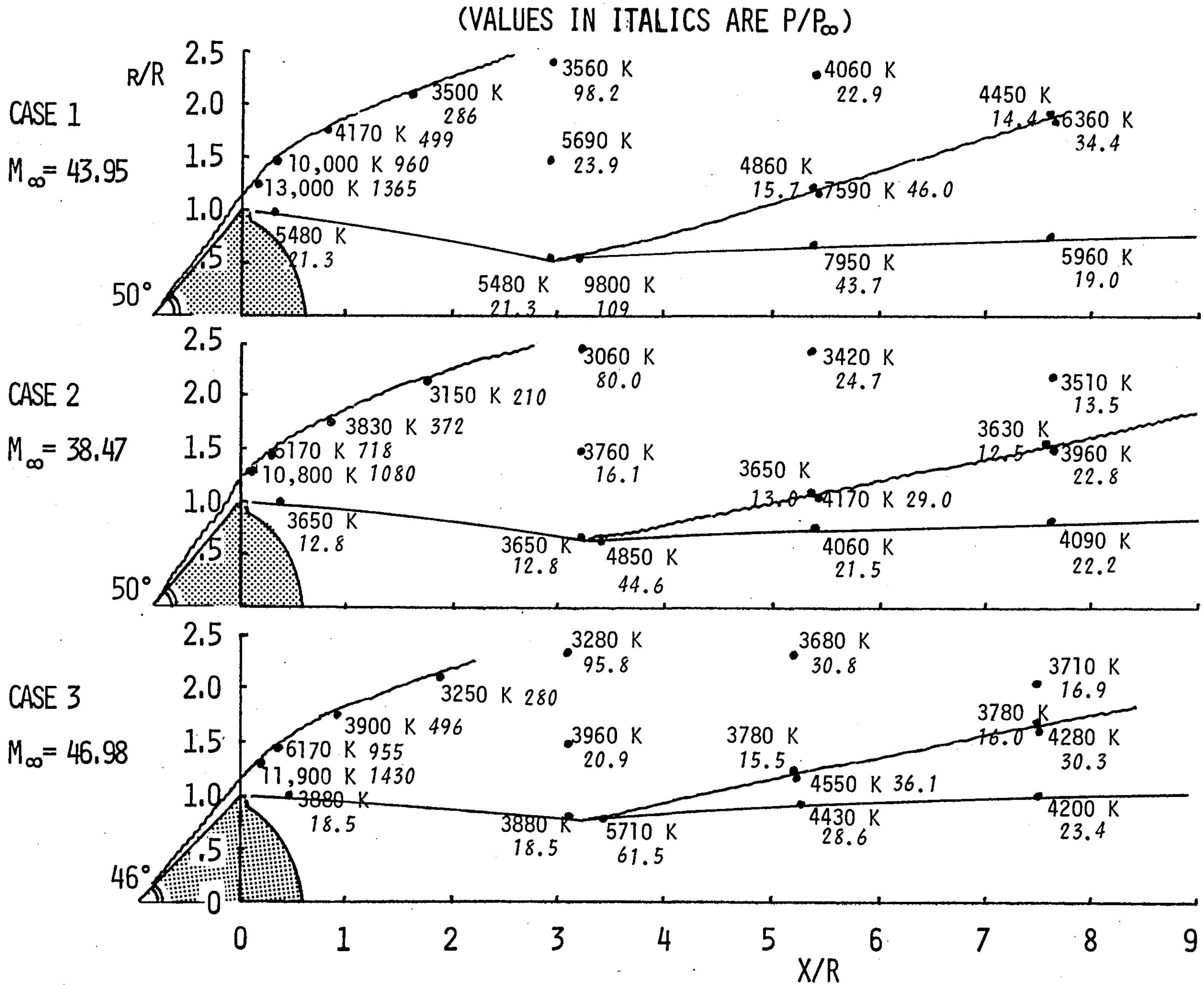

Fig. 16 Comparison of Inviscid Wakes

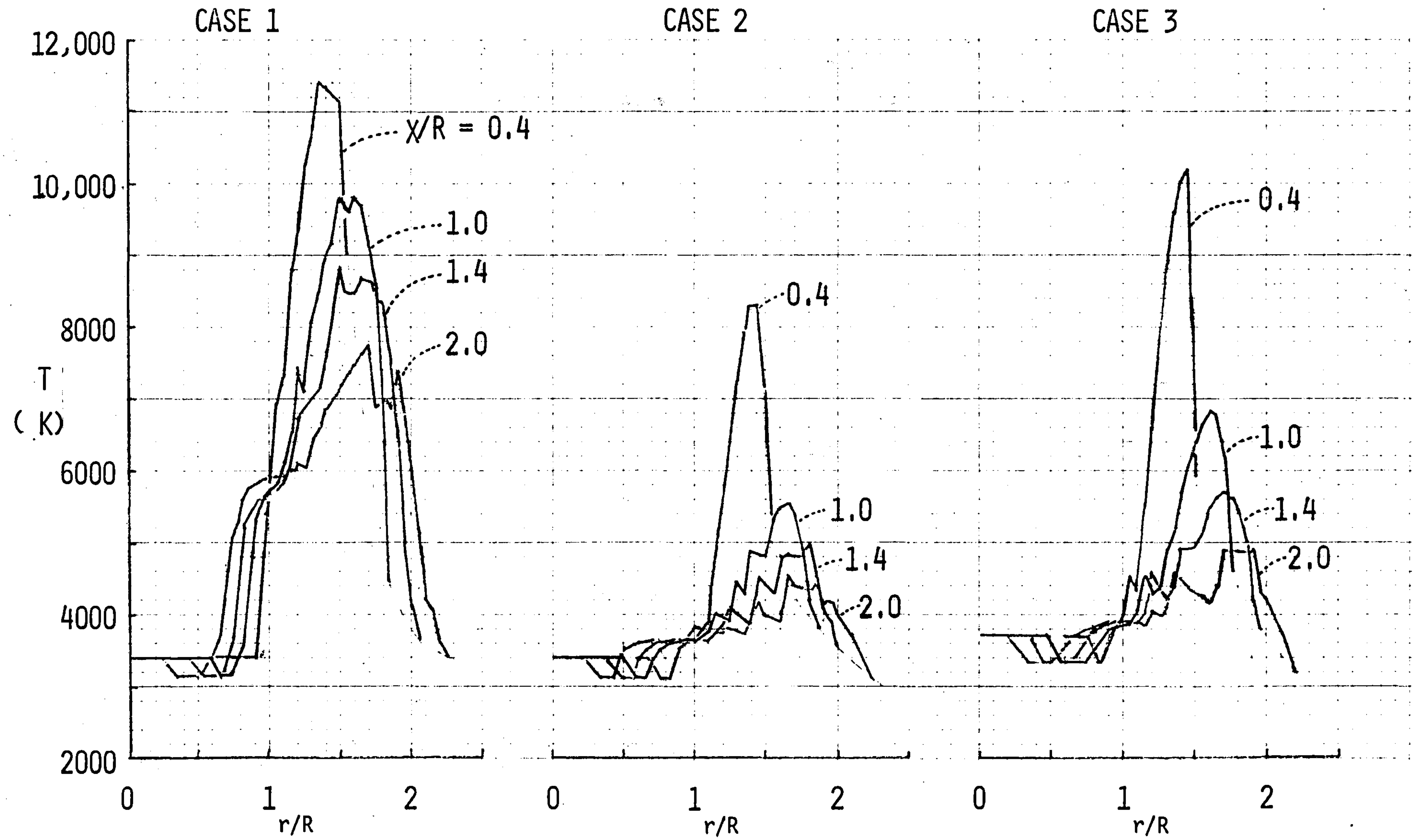

Fig. 17 Near Wake Radial Temperature Profiles

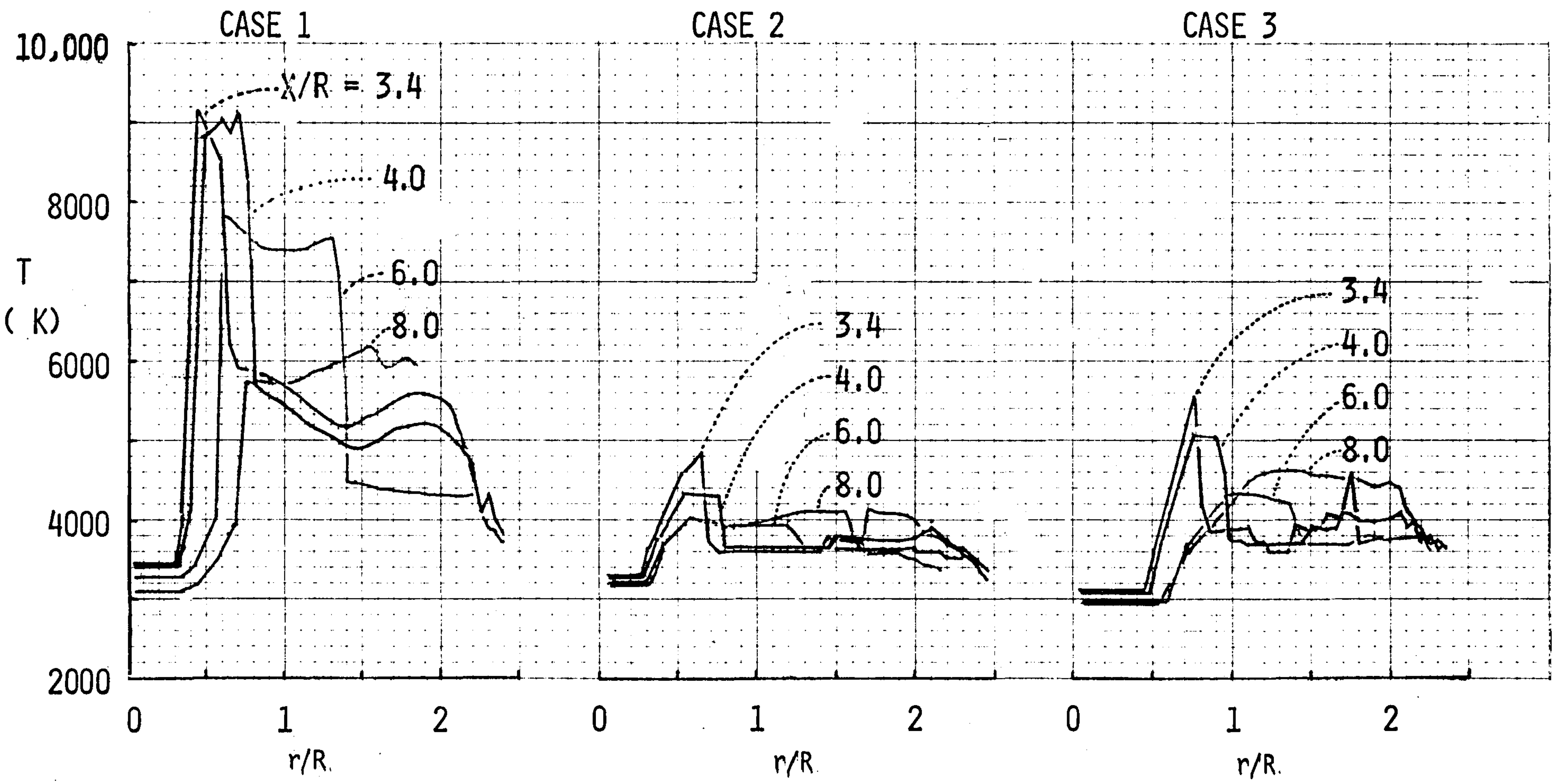

Fig. 18 Far Wake Radial Temperature Profiles

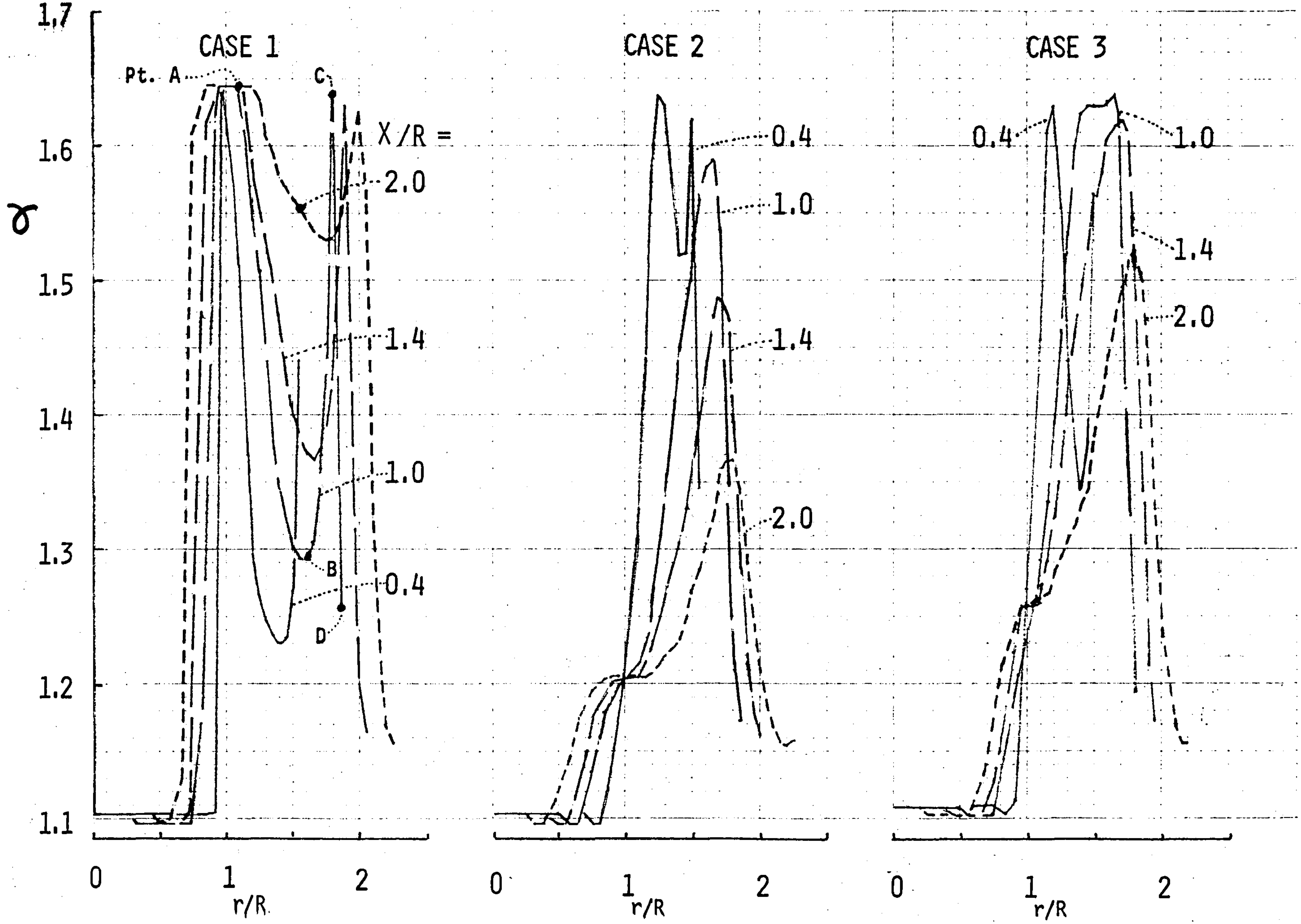

Fig. 19 Near Wake Radial Gamma Profiles

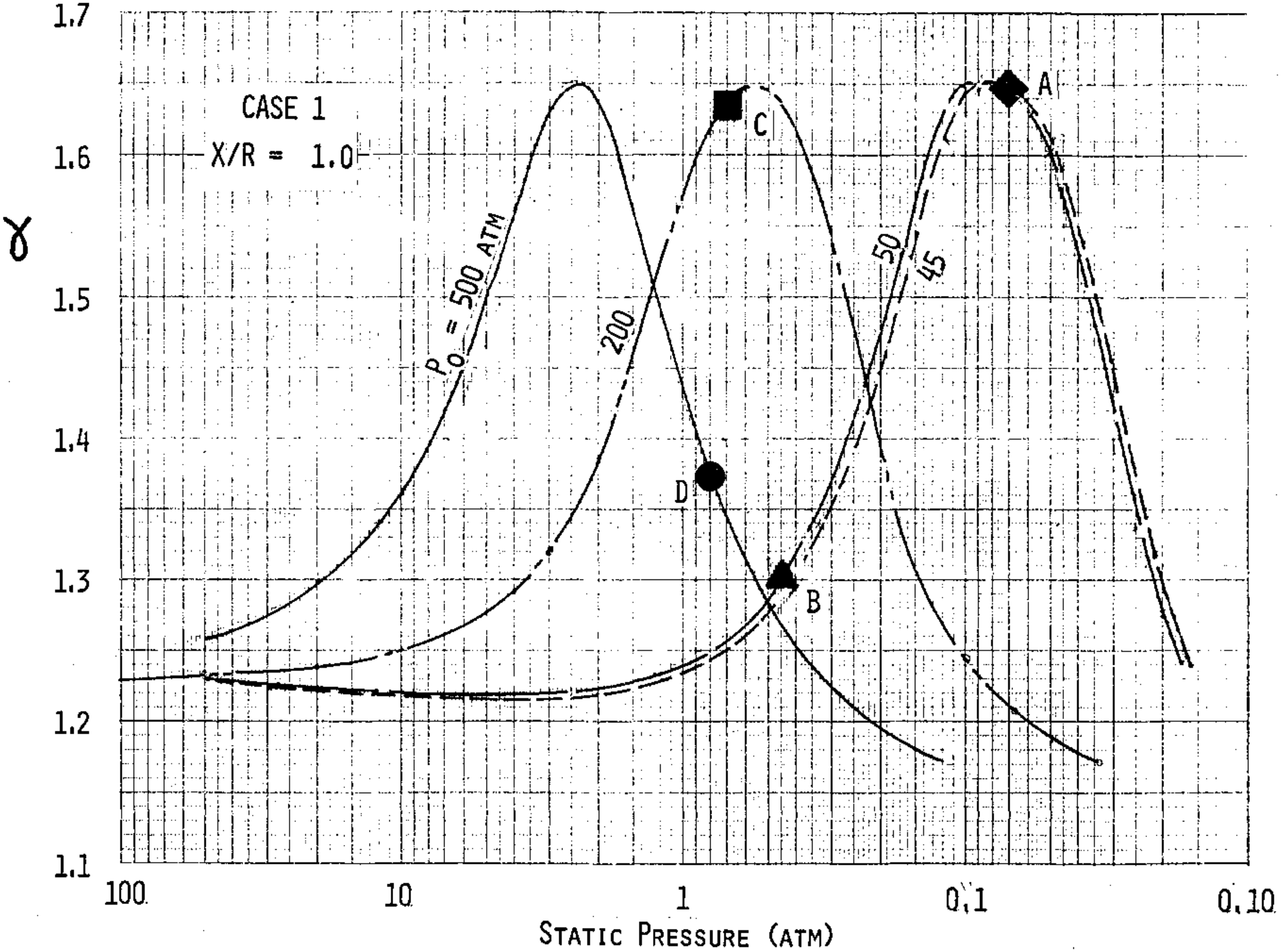

Fig. 20 Gamma Variation with Total and Static Pressure

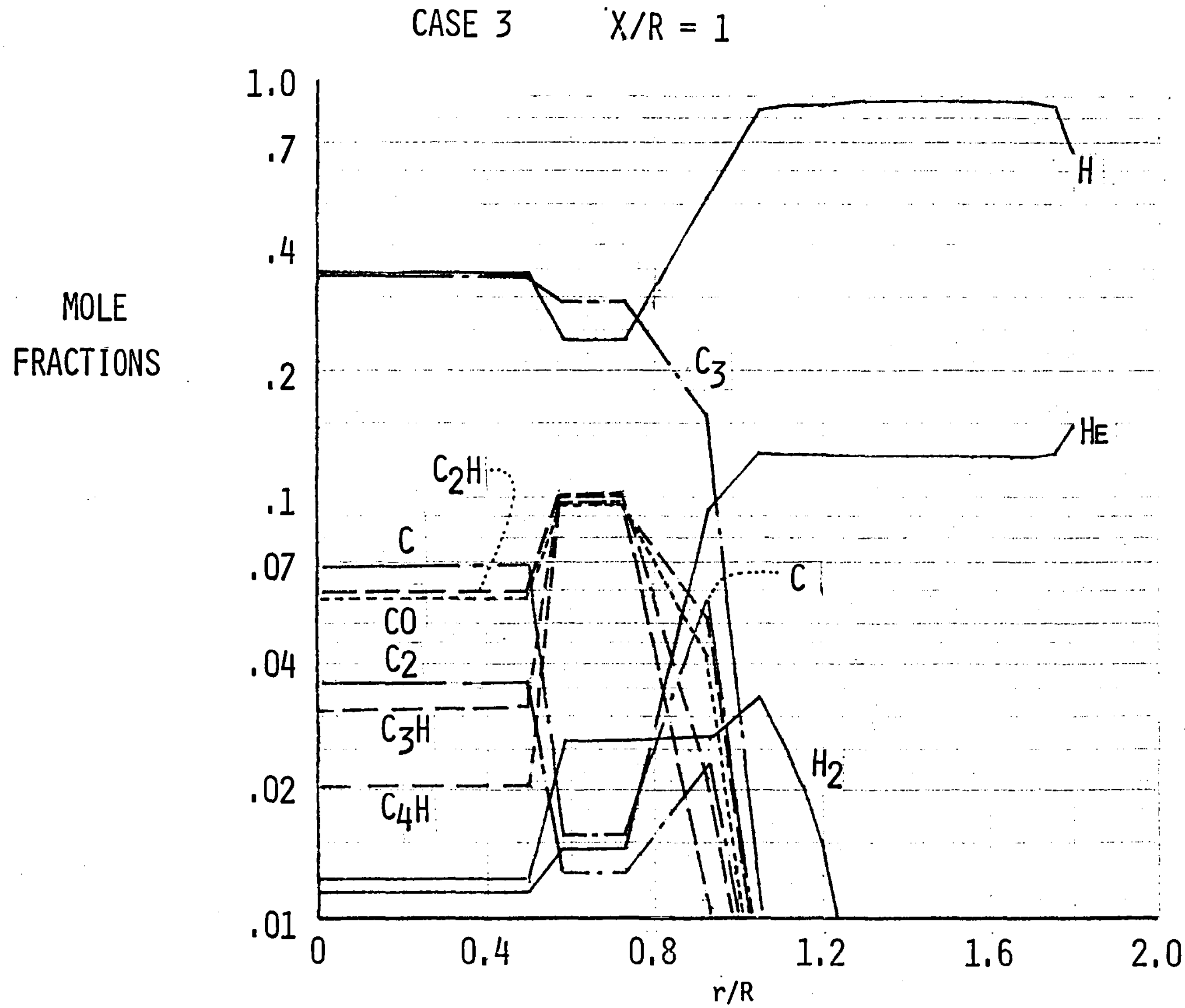

Fig. 21 Near Wake Mole Fraction Profiles

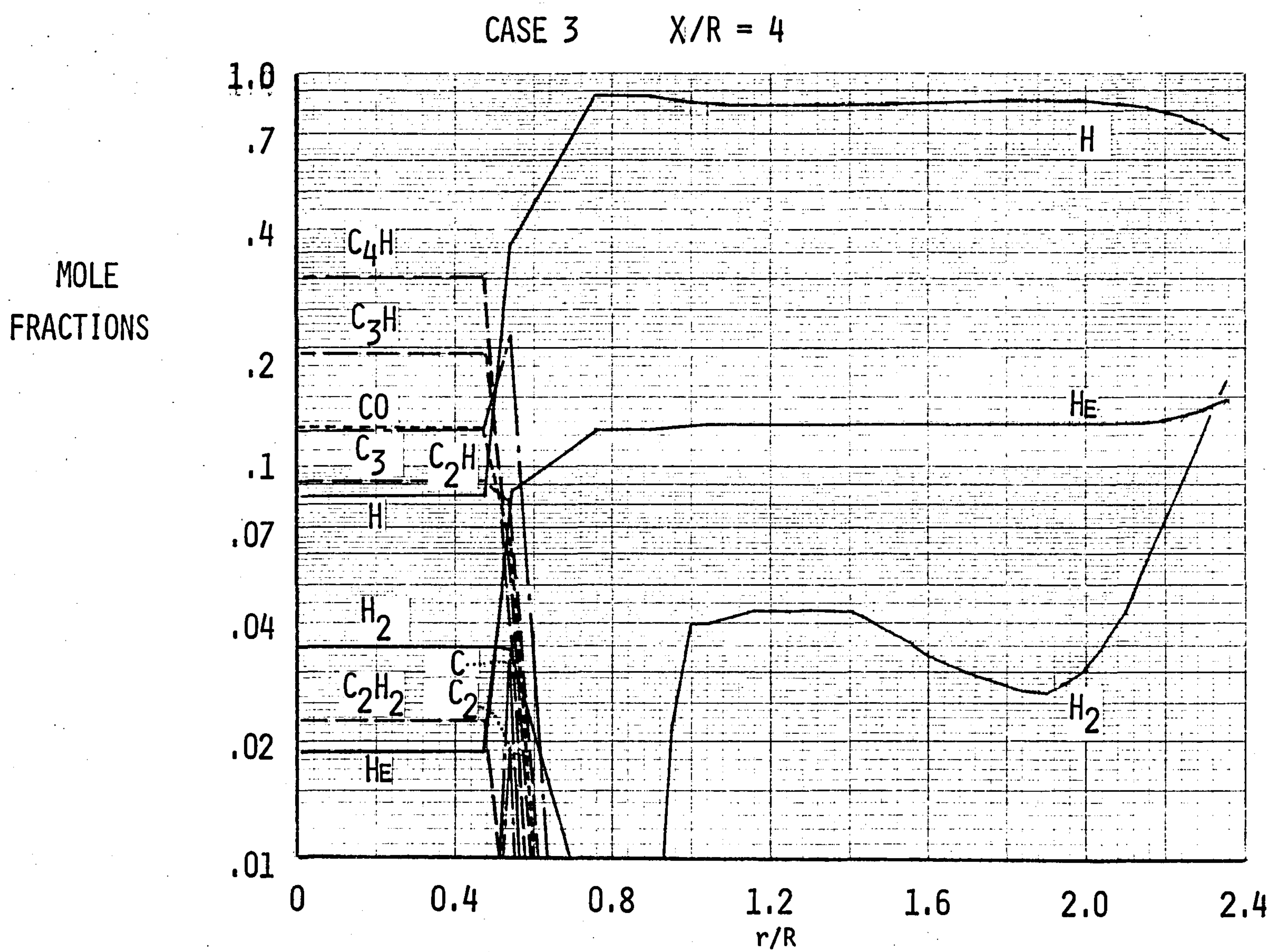

Fig. 22 Far Wake Mole Fraction Profiles

Section 4.0

CONCLUSIONS AND RECOMMENDATIONS

Based on the analysis and results of this study, the following conclusions are drawn.

(1) The wake geometry used is consistent with recent Jovian probe shadowgraphs.

(2) The wake geometry is sensitive to P_B/P_∞.

(3) Case 1 produced the highest flowfield temperature and pressure ratios.

(4) The complex real gas processes in the flowfield preclude attempts of obtaining an effective gamma for experimental work.

(5) The C_3 species is a dominant species in the near viscous wake, whereas, C_4H and C_3H are more dominant in the far viscous wake.

As a consequence of the information obtained in this study, the following recommendations are made.

(1) Shear layer calculations should be axisymmetric and account for nonparallel inviscid flow.

(2) An improved recirculation model should be developed.

(3) A variable pressure near wake model is required for accurate neck region calculations.

(4) Addition range tests to obtain higher quality shadowgraph photos of the wake geometry would improve confidence in modeling work.

(5) Base pressure measurements for the probe configuration would significantly increase the confidence in current calculation methods.

Section 5.0

REFERENCES

(1) Moss, J. N. and A. L. Simmonds, "The Impact of Turbulence on a Radiating Shock Layer with Coupled Ablation Injection," AIAA Paper No. 78-1186, July 1978.

(2) Moss, J. N., J. J. Jones and A. L. Simmonds, "Radiative Flux Penetration Through a Blown Shock Layer for Jupiter Entry," AIAA Paper No. 78-908.

(3) Gordon, S. and B. J. McBride, "Computer Program for Calculation of Complex Chemical Equilibrium Compositions, Rocket Performance, Incident and Reflected Shocks, and Chapman-Jouguet Detonations," NASA SP-273, February 1973.

(4) Smith, S. D. and A. W. Ratliff, "Rocket Exhaust Plume Computer Program Improvement," LMSC-HREC D162220, Lockheed Missiles and Space Company, June 1971.

(5) Lees, L., "Hypersonic Wakes and Trails," AIAA Journal, Vol. 2, No. 3, March 1964, pp. 417-428.

(6) Reeves, B. L., and L. Lees, "Theory of Laminar Near Wake of Blunt Bodies in Hypersonic Flow," AIAA Journal Vol. 3, No. 11, November 1965, pp. 2061-2074.

(7) Smith, C. E., R. L. Dramer and A. C. Brown, "A Study of the Laminar Near-Wake Behind a Cylinder at Mach 20," AIAA Journal, Vol. 4, No. 7, July 1966, pp. 1188-1194.

(8) Vas, I. E., E. Murman and S. M. Bogdonoff, "Studies of Wakes of Support-Free Spheres at M = 16 in Helium," AIAA Journal, Vol. 3, No. 7, July 1965, pp. 1237-1244.

(9) Dewey, C. F., Jr., "Near Wake of a Blunt Body at Hypersonic Speeds," AIAA Journal, Vol. 3, No. 6, June 1965, pp. 1001-1010.

(10) Wagner, R. D., "Measured and Calculated Mean-Flow Properties of a Two-Dimensional Hypersonic, Turbulent Wake," TN D-6927, November 1972, NASA.

(11) McCarthy, J. F., Jr., and T. Kubota, "A Study of Wakes Behind a Circular Cylinder at M = 5.7," AIAA Journal, Vol, 2, No. 4, April 1964, pp. 629-636.

(12) Brant, D. N., and D. E. Nestler, "Development of an Afterbody Radiative and Convective Heating Code for Outer Planet Probes," AIAA Paper 78-862, May 1978.

(13) Park, C., "Modeling of Radiative Heating of Base Region of Jovian Entry Probe," AIAA Paper 79-0039, January 1979.

(14) Audeh, B. J., "Equilibrium Shear Layer Program," TM 54/20-169, Lockheed Missiles & Space Company, December 1967.